SOX10 as a novel target in melanoma: a proteomics-based approach to expanding druggability

Doctoral thesis

to obtain a doctorate (Dr. med)

from the Faculty of Medicine

of the University of Bonn

Kira Vordermark

from Würzburg

2025

Written with authorization of the
Faculty of Medicine of the University of Bonn

First reviewer: Prof. Dr. med. Ingo Schmidt-Wolf

Second reviewer: Prof. Dr. med. Eleni Gkika

Day of oral examination: January 17, 2025

From the Department of Integrated Oncology

Table of contents

List of abbreviations

ANOVA	ANalysis Of Variance
ACSS1	Ayl-CoA synthetase short chain family member 1
AJCC	American Joint Committee on Cancer
AP2α	activator protein 2 alpha
BRAF	v-Raf murine sarcoma viral oncogene homolog B
BP	base pair
CDM	cysteine druggability mapping
CI	confidence interval
CTLA-4	cytotoxic T-lymphocyte-associated cell death 4
CD	cluster of differentiation
ChIP-seq	chromatin immunoprecipitation sequencing
CRISPR	clustered regularly interspaced short palindromic repeats
DBIA	iodoacetamide-desthiobiotin
DCT	dopachrome tautomerase
DEPMAP	The Cancer Dependency Map (by Broad Institute)
DMEM	Dulbecco's Modified Eagle's Medium
DMSO	dimethyl sulfoxide
DNA	deoxyribonucleic acid
EGFR	epidermal growth factor
ESMO	European Society for Medical Oncology
FOXD3	forkhead box D3
GAS7	growth arrest-specific protein 7
GATA-3	GATA binding protein 3
GLUC	Gaussia luciferase
GPCR	G-protein coupled receptor
HMB-45	human melanoma black 45
HSPD1	heat shock protein family D member 1
HSPE1	heat shock protein family E member 1
ICD-10	International Classification of Disease 10
MAPK	mitogen-activated protein kinase

MEK	MAPK kinase
MIA	melanoma inhibitory activity
MITF	microphthalmia-associated transcription factor
NCCN	National Comprehensive Cancer Network
PAX3	paired box gene 3
PD-1	programmed cell death 1
PD-L1	programmed cell death ligand 1
RNA	ribonucleic acid
RAB7A	ras-associated protein 7A
RNF144A	ring finger protein 144A
RT	room temperature
RXRG	retinoid x receptor gamma
SDS-PAGE	sodium dodecyl sulfate polyacrylamide gel electrophoresis
SEAP	secreted embryonic alkaline phosphatase
siRNA	small interfering RNA
SOX10	SRY (sex determining region y)-box 10
SNL	sentinel lymph node
TRPM1	transient receptor potential cation channel subfamily M member 1
TYR	tyrosinase
TYRP1	tyrosinase-related protein 1
UICC	Union Internationale Contre le Cancer
WT	wild type
ZfKD	Zentrum für Krebsregisterdaten = German Center for Cancer Registry Data

1. Introduction

1.1 Melanoma epidemiology

Melanoma of the skin, listed as C43 in the International Classification of Disease (ICD) - 10, is an aggressive malignant neoplasm that arises from uncontrolled proliferation of melanocytes (Matthews et al., 2017; Tang and Cao, 2021).

In Germany, the most recent report of the German Center for Cancer Registry Data (Zentrum für Krebsregisterdaten, ZfKD) from 2023 gives an overview of the tumor´s epidemiologic dynamics up to the most recent time period from 2019 to 2020. In 2020, 23,560 people were diagnosed with melanoma of the skin, 11,320 of those being women. The average age at melanoma onset was 63 years for women, and 69 years for men. According to the report, the age-standardized incidence rate of both genders rose dramatically in 2008 after the establishment of the nationwide skin cancer screening. Since 2012, the incidence in women has been slightly decreasing, whereas that reported in men has been stabilizing. Mortality rates, however, have barely changed since 1999 (RKI, 2023). This can be attributed to an earlier detection of tumors with a good prognosis (Leitlinienprogramm Onkologie, 2020).

The clinical outcome of melanoma depends on the stage at diagnosis and can be estimated based on 7^{th} and 8^{th} edition TNM-staging and grouping according to the Union Internationale Contre le Cancer (UICC) from 2016. To show cancer-dependent mortality, relative 5-year survival rates are calculated. The relative 5-year survival rate equals the ratio of absolute survival (i.e. the number of alive patients five years after diagnosis divided by the total number of diagnosed patients) divided by the expected survival of the general population of the respective age and sex. For example, a relative 5-year survival rate of 100% implies that within five years of being diagnosed with cancer, the number of diagnosed patients who died equals the number of those people who were expected to die based on survival rates in the respective population.

While the prognosis remains excellent for patients presenting with localized, node-negative disease (UICC I, II) with relative 5-year survival rates amounting to 102 % in women, 105 % in men (UICC stage I), and 83 % in women and 79 % in men (UICC stage II), the corresponding chances of survival drop drastically in advanced stages. Once tumor growth involves regional lymph nodes (UICC stage III), 5-year survival rates amount to 75 % in women and 69 % in men; after spreading to distant lymph nodes or organs (UICC stage IV), relative 5-year survival rates reach 41 % in women and 40 % in men (RKI, 2023).

Although melanoma accounts for only about 1% of all skin cancers, it is responsible for the vast majority of skin-cancer related deaths and shows the highest rate of metastasis across all skin cancers (Cheng et al., 2018). Distant metastases typically localize to the liver, lung, and brain. It follows that advanced melanoma is a serious, potentially lethal disease with a considerable metastatic potential that requires unprecedented efforts to improve patient outcomes, in particular overall survival and progression-free survival.

Melanoma can be subdivided into 1) lentiginous melanoma, 2) superficial spreading melanoma, 3) nodular melanoma and 4) acral lentiginous melanoma types. Superficial spreading melanoma is the most common subtype (60-70 %), marked by slow, horizontal tumor growth, which makes it detectable early on and, hence, is linked to a favorable prognosis. However, other subtypes such as nodular (20-30 %) melanoma are characterized by a more accelerated vertical growth, thus leading to a poor prognosis. Less frequently diagnosed subtypes of melanoma include lentigo maligna melanoma (~10 %), which usually progresses slowly from lentigo maligna disease to the malignant tumor and acral lentiginous (~5 %) melanoma which can be characterized by slow horizontal growth with predilection sites not easily visible, e.g. the sole of the foot (Göhl et al., 2009).

The primary acquired risk factor for melanomagenesis is exposure to ultraviolet radiation, including both natural and artificial sunlight, the exposition to which has increased within the past decades. Innate risk factors include 1) phenotypic predisposition, e.g., fair complexion, atypical or dysplastic mole pattern, 2) personal medical history or comorbidities, i.e. multiple sunburns, and rarely, inherited skin conditions (i.e. rare genodermatoses like

xeroderma pigmentosum) 3) genetic predisposition, e.g., positive family history of (cutaneous) melanoma (National Comprehensive Cancer Network, 2024).

1.2 Melanoma stage IV state-of-the-art treatment and its limitations

Importantly, 42-45 % of melanomas harbor mutations of the gene for v-Raf murine sarcoma viral oncogene homolog B (BRAF), which is an activating serine / threonine protein kinase in the mitogen-activated protein kinase (MAPK / MEK) signaling pathway. Most commonly, V600 is either substituted for glutamate (V600E, accounting for ~80 % of all BRAF mutations) or lysine (V600L, accounting for ~16 % of all BRAF mutations) which renders the protein and downstream RAF-MEK-ERK signaling constitutively active and detached from physiological regulation. BRAF V600 mutations are associated with sensitivity to BRAF and MEK inhibitors and both recent NCCN and European Society for Medical Oncology (ESMO) guidelines recommend molecular testing for stage-IV tumors in order to determine the therapeutic strategy (Michielin et al., 2019; National Comprehensive Cancer Network, 2024). Small molecule inhibitors targeting BRAF (i.e. the ATP-binding pocket of active confirmation of BRAF) - namely vemurafenib, dabrafenib, encorafenib - and its downstream effector MEK - such as cominitib, trametinib, binimetinib - have achieved great success in the medical treatment of BRAF-mutant melanoma (Subbiah et al., 2020).

According to the National Comprehensive Cancer Network (NCCN) of the United States, preferred first-line therapy regimens for the treatment of unresectable or distant metastatic disease include both targeted therapy and immunotherapy (National Comprehensive Cancer Network, 2024). Cytotoxic therapies are not preferred but can be useful in patients that are not eligible for standard first-line treatment options, for example because of comorbidities. German guidelines recommend using either a BRAF-inhibitor paired with a MEK-inhibitor or an immune checkpoint inhibitor, the latter of which can be either PD-1 monotherapy or anti-PD-1 plus anti-CTLA-4 antibodies (Leitlinienprogramm Onkologie, 2020).

A combination of BRAF- and MEK- inhibitors in the treatment of metastatic melanoma was shown to be superior to monotherapy with a BRAF inhibitor in phase III clinical trials:

dabrafenib + trametinib (Robert et al., 2019a), vemurafenib + cobimetinib (Ascierto et al., 2016), encorafenib + binimetinib (Dummer et al., 2018). Consequently, these three combination target therapies are now recommended for BRAF V600-mutation-positive cancers (National Comprehensive Cancer Network, 2024). Despite survival advantages when compared to chemotherapy, melanoma patients´ benefit is limited by short-lived responses and acquisition of resistance (via heterogeneous mechanisms, typically in MAPK signaling), resulting in disease progression within six to seven months of initiation of treatment with dabrafenib or vemurafenib (Subbiah et al., 2020).

Melanoma is a highly immunogenic tumor for which both the existence of lymphocytic infiltrates in primary tumors and metastases and the recognition of melanoma antigens by tumor-infiltrating T lymphocytes have been reported. Recent advances in immunotherapy have yielded several promising treatment options for melanoma patients: First, biological immunotherapy including cytokines, interferons and granulocyte-monocyte colony stimulating factors; second, cancer vaccines either targeting melanoma cells directly or via a dendritic cell-based, peptide-based or vector-based approach; third, adoptive cell transfer and last, immune checkpoint inhibitors (Rodríguez-Cerdeira et al., 2017).

Immune checkpoints are often exploited by melanoma cells to decrease anticancer immune activity and escape tumor recognition mechanisms. The identification of specific targets within that dysfunctional immune system such as programmed cell death protein 1 (PD-1) and cytotoxic T-lymphocyte-associated protein 4 (CTLA-4) led to the development of respective checkpoint inhibitors including anti-CTLA-4 monoclonal antibodies (ipilimumab and tremelimumab), anti-PD-1 (pembrolizumab, pidilizumab, nivolumab), and anti-PD-L1-antibodies (atezolizumab, avelumab, durvalumab), fostering cancer cell killing mediated by cluster of differentiation (CD) 8-positive T cells.

The five-year follow-up of advanced melanoma patients previously enrolled in a phase III study comparing pembrolizumab with ipilimumab found both the median overall survival and progression-free survival to be superior in the pembrolizumab groups over the ipilimumab one (Robert et al., 2019b): Combined data of the pembrolizumab treatment groups (every two or three weeks for 24 months) showed a median overall survival of 32.7

months (95 % CI 24.5-41.6) and a median progression-free survival of 8.4 months (95 % CI 6.6-11.3), compared to only 15.9 months (95 % CI 13.3-22.0) and 3.4 months (95 % CI 2.9-4.2), respectively, in the ipilimumab arm.

A similar phase III trial - CheckMate 067 - was able to compare five-year outcomes of nivolumab versus ipilimumab monotherapy versus nivolumab-plus-ipilimumab combination therapy. The median overall survival was 36.9 months (95 % CI, 28.2 to 58.7) in the nivolumab groups, as compared with 19.9 months (95 % CI, 16.8 to 24.6) in the ipilimumab group. More importantly, in the nivolumab-plus-ipilimumab group, the median overall survival was more than 60 months (median not reached; 95 % CI, 38.2 to not reached) (Larkin et al., 2019).

Currently, there are two drawbacks concerning immunotherapy in melanoma. First, durable responses are seen in merely 30 to 40 % with monotherapy, or up to 60 % with combination therapy (Jessurun et al., 2017). Second, across all studies, checkpoint blockade therapy resulted in immune-related adverse events. Because they typically affect multiple organs or systems, primarily the skin, gastrointestinal tract, lungs, thyroid and endocrine system, and have the potential to become life-threatening, efficacy of checkpoint blockade is limited by immune-related adverse events, e.g., when medication must be discontinued. In 2024, combination checkpoint blockades, i.e. nivolumab / ipilimumab and nivolumab / relatlimab-rmbw, are preferred over anti-PD1-monotherapies. However, in patient counseling, a higher risk of immune-related adverse events mentioned in combination therapy must be taken into account (National Comprehensive Cancer Network, 2024).

Three important clinical trials have explored the combination of targeted therapy and immunotherapy, i.e. BRAF- or MEK-inhibitor with either anti-PD1- or anti-PD-L1-antibody, in advanced BRAF-mutant melanoma (Trojaniello et al., 2023). In KEYNOTE-022, a phase-I/II clinical trial, patients received dabrafenib and trametinib daily with pembrolizumab 3-weekly, or with placebo. Median progression-free survival, the primary endpoint in all three studies, was 16.9 in the triple therapy arm versus 10.7 months in the placebo arm, although not statistically significant (Ferrucci et al., 2020). IMspire150 / TRILOGY compared vemurafenib with cometinib plus atezolizumab, or plus placebo. A statistically significant

increase in median progression-free survival, 15.1 versus 10.6 months, was observed (Gutzmer et al., 2020). Lastly, in COMBI-I, another phase III clinical trial, the experimental arm consisted of dabrafenib and trametinib plus spartalizumab daily, the standard arm of dabrafenib and trametinib plus placebo, resulting in median progression-free survival of 16.2 versus 12.0 months (Nathan et al., 2020). Across all three clinical trials, the rate of high-grade (grade 3 to 5) adverse events increased in the combination arms, for example in KEYNOTE-022, 58.3 % in the triplet arm vs. 25 % in the standard treatment arm, respectively. Adverse events included fever, rash, and liver transaminase elevation.

According to the German S3 guidelines, no conclusive data is available regarding the sequential therapy of immunotherapy and targeted therapy (Leitlinienprogramm Onkologie, 2020). However, several trials are currently investigating the most efficient sequence when combining targeted therapy and immunotherapy (Trojaniello et al., 2023). Preliminary results suggest placing the immune checkpoint inhibitors first leads to a clinical advantage, whereas administering immunotherapy after a course of targeted therapy decreases their efficacy. For example, in the phase-III trial DREAMSeq (Doublet, Randomized Evaluation in Advanced Melanoma Sequencing), treatment-naïve patients received either nivolumab / ipilimumab (arm A) or dabrafenib / trametinib (arm B) , followed at progression by either dabrafenib / trametinib (arm C) or nivolumab / ipilimumab (arm D). Median PFS after progression was 9.9 months (95 % CI, 8.3 to 20.8) in arm C and 2.9 months (95 % CI, 2.6 to 8.9) in arm D (Atkins et al., 2023).

To conclude, there have been advances in melanoma treatment by combining targeted therapy and immunotherapy. However, developing novel treatment approaches remains an area of critical need to lower melanoma-associated mortality rates. To identify advanced treatment targets, genetic studies have explored genes responsible for tumorigenesis in melanoma, but inhibition of target proteins with small-molecule drugs continues to be challenging.

1.3 Covalent inhibitors targeting cysteine residues - a promising treatment approach

Across all cancer types, presently only about 20 % of all oncogenic drivers have been targeted pharmacologically which are mainly enzymes like kinases and G-protein coupled receptors (GPCRs). However, most cancer drivers are considered “undruggable”, accounting for the less tractable transcription factors, protein-protein interactions, scaffolds as well as small GTPases.

To expand the number of druggable gene products, covalent inhibitors are used. By establishing a covalent bond to specifically target proteins through a reactive functional group, covalent inhibitors offer increased affinity over traditional, non-covalent drug binding (Boike et al., 2022). Covalent inhibitors offer certain advantages over the traditional non-covalent ligand design (Maurais und Weerapana, 2019). First, covalent inhibitors can target shallow binding pockets that are uncooperative towards non-covalent inhibitors. Second, covalent inhibitors are characterized by high potency and long binding duration. It follows that necessary dose and intake frequency are lower compared to normal drugs (Copeland, 2016). Lastly, with the lower dosing frequency achieved, patient compliance increases (Sutanto et al., 2020).

Disadvantages of covalent inhibitors are off-target effects, induced by reactive compounds binding to amino acids other than the intended one, and immune responses, triggered by foreign-appearing compound-protein complexes (Sutanto et al., 2020).

Covalent inhibitor research has given rise to multiple, as of today FDA-approved anticancer drugs, such as chemotherapeutics bortezomib (2003), ibrutinib (2013) and dacomitinib (2018). Ibrutinib - a drug used to treat B-cell malignancies - covalently binds cysteine residue C481 provoking an irreversible inhibition of Bruton’s tyrosine kinase (BTK). Similarly, osimertinib - approved for the treatment of non-small cell lung cancer - binds irreversibly, via the C797 amino acid covalent bond, to certain sensitizing mutant forms of epidermal growth factor (EGFR) (Zhang, 2016).

Within the human proteome, cysteine residues have proven to be particularly promising to target. For one, they are concentrated at key functional sites within proteins and therefore play critical roles, i.e., by acting as nucleophiles in enzyme active sites, modifying proteins post-translationally, coordinating metal and lipid binding and mediating protein / protein interactions. In addition, because of their nucleophilicity under physiological conditions, caused by an aliphatic thiol (SH), cysteine residues constitute ideal anchoring sites for electrophilic small molecules. Cysteine residues are therefore preferred over the 19 remaining canonical amino acids when finding potential sites for covalent drug development.

1.4 Defining druggable cysteine content by cysteine druggability mapping

There are two approaches to discover novel covalent inhibitors. Traditionally, reactive, electrophilic groups have been incorporated into a ligand to achieve covalent, i.e. non-reversible, binding. More recently, an “electrophile-first approach” has been established in which electrophilic ligands are identified by screening libraries of electrophilic compounds (Boike et al., 2022). Herein, covalent ligand screening was employed.

To define those nucleophilic cysteine residues that are amenable to electrophilic covalent small molecule inhibition, the laboratory of Liron Bar-Peled, PhD, previously developed a method called Cysteine Druggability Mapping (CDM). CDM profiles small-molecule cysteine interactions on a whole-proteome scale. Cysteine reactive drug-like fragments (“scout fragments” or “drug probes”) are employed. Three scout fragments, KB02, KB03 and KB05 (**Figure 1**) were chosen from a library and recapitulate their ligandability at about 70%. Scout fragments interact with reactive cysteines by forming covalent adducts (Bar-Peled et al., 2017; Vinogradova and Cravatt, 2021). Next, only those cysteines that interacted with scout fragments can escape a treatment with a pan-cysteine-reactive probe (iodoacetamide-desthiobiotin, DBIA). Candidate targets identified by CDM were defined as those cysteines that were engaged by drug probes but not by the control molecule. Cysteines were called “ligandable” when they engaged > 60 % by cysteine-reactive compounds. Preliminary experiments performed in the Bar-Peled Lab demonstrated that

cysteines bound at high occupancy with drug probes are significantly more amenable to inhibition with advanced covalent inhibitors.

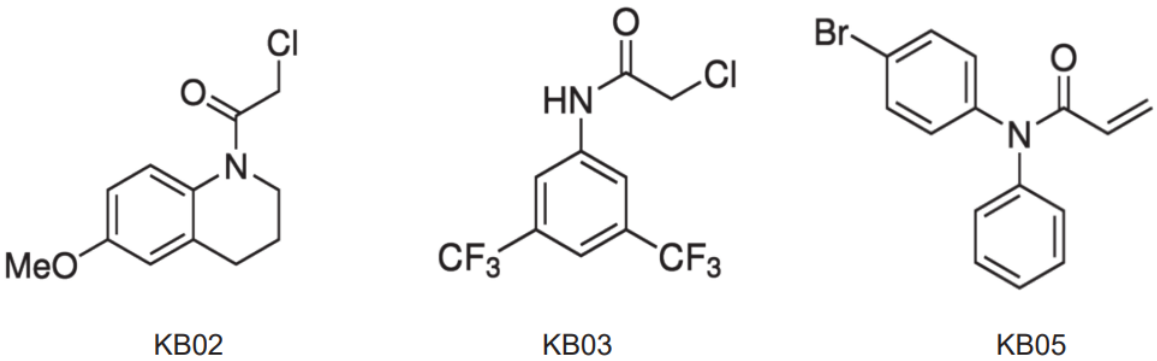

KB02 KB03 KB05

Figure 1: Electrophilic scout fragments for targetable cysteines KB02, KB03 and KB05 were employed to evaluate cysteine reactivity and ligandability. KB02/KB03/KB05 = C 2-Chloro-1-(6-methoxy-3,4-dihydroquinolin-1(2H)-yl)ethan-1-one/// N-Chloroacetyl-3,5-bis(trifluoromethyl)aniline///*N*-(4-Bromophenyl)-*N*-phenylacrylamide

1.5 A melanoma drug map identifies SOX10 and MITF-M

When melanoma cell line SK-MEL2 was processed by Cysteine Druggability Mapping, a cysteine inhibition at ~80 % in Sry-related HMG-box (SOX10) and ~50 % in M-MITF, isoform M of Microphthalmia-Associated Transcription factor (MITF) was observed, both of which are lineage-specific transcription factors **(Figure 2a)**. One cysteine in SOX10, C71, and two cysteines in MITF, C160 and C413, were identified as highly ligandable **(Figure 2b, c)**.

The Cancer Dependency Map initiative at the Broad Institute of Massachusetts Institute of Technology and Harvard University (DEPMAP) had shown SOX10 to be essential for growth in almost all melanoma cell lines. In addition, MITF was among SOX10´s top three codependencies both according to clustered regularly interspaced short palindromic repeats (CRISPR) (Pearson´s correlation coefficient ρ = 0.50; DepMap Public 22Q4+Score,

Chronos)) and RNA interference (RNAi) data (ρ = 0.49; Achilles+DRIVE+Marcotte, DEMETER2). When comparing proteins identified as druggable in melanoma by CDM (total 2346 proteins) with genes classified as essential for melanoma growth by the Cancer Dependency Map (total 38 genes), the resulting overlap of 17 included, among BRAF, transcription factor SOX10 (Broad Institute, 5/17/2024).

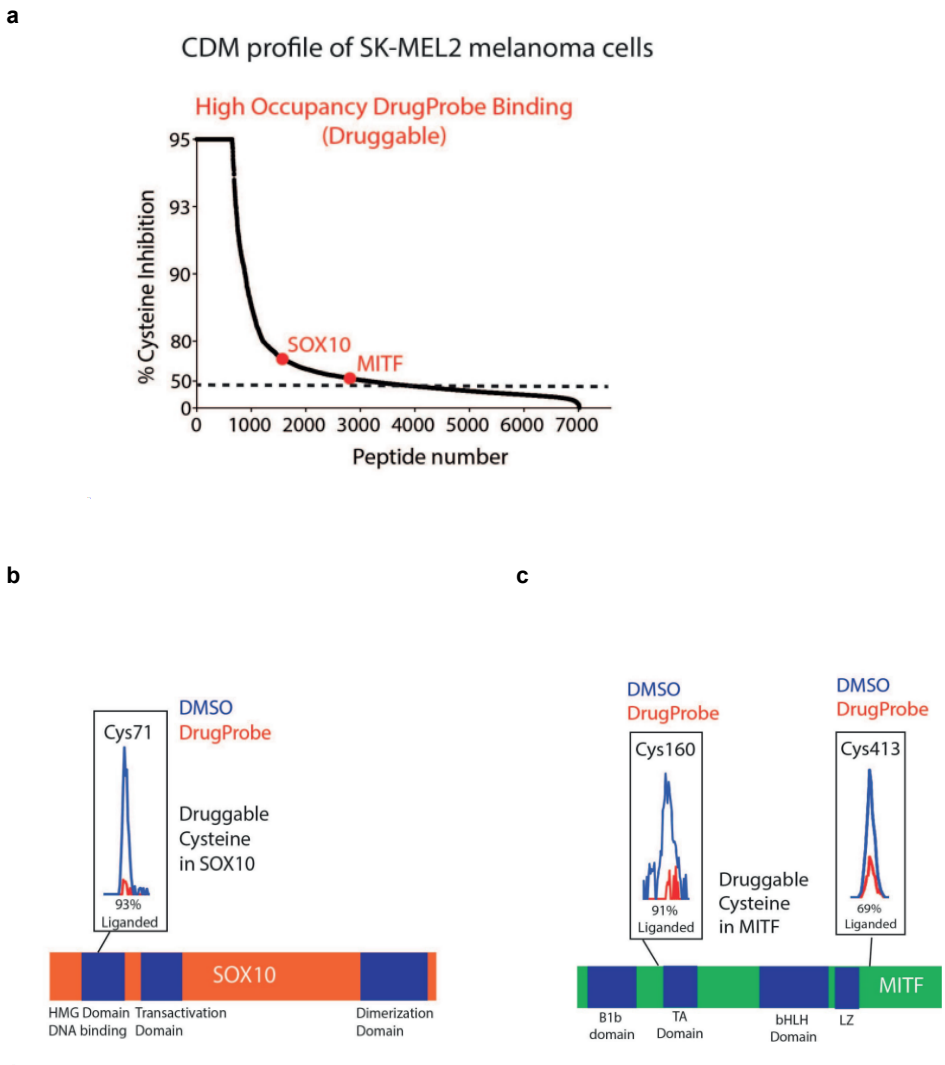

Figure 2: Cysteine druggability mapping identifies druggable cysteine residue in transcription factor SOX10
Data from Liron Bar-Peled, PhD, and Mariko Hara, PhD (with permission).

a, Cysteine druggability mapping in SK-MEL2 cells revealed cysteine inhibition at around 80% in SOX10 whereas cysteines of MITF were inhibited at more than 50%. **b,** one cysteine in SOX10 and **c**, two cysteines in MITF were identified as highly ligandable.

1.6 Transcription factor SOX10 and how it is linked to melanoma

SOX10 belongs to the SOX family of transcription factors all of which share the same 79-amino acid DNA-binding domain with homology to the high mobility group (HMG) box of SRY (sex-determining region Y; hence SOX10, Sry bOX) (Pingault et al., 2022). Based upon the homology of this high-mobility group (HMG) domain, twenty mammalian SOX factors are divided into nine subfamilies (A, B1, B2-H) (Bowles et al., 2000), SOX10 belongs to SOXE. All SOX family members are able to recognize a consensus 7 bp consensus element: (A/T) (A/T) CAA (A/T) G (Peirano and Wegner, 2000). Additionally, an inverted repeat motif, two SOX family motifs separated by four nucleotides, was identified by chromatin immunoprecipitation sequencing (ChiP-Seq), suggesting that SOX family proteins often regulate gene expression by dimerization (Fufa et al., 2015).

SOX10 has been studied extensively as a key player in both the development of the neural crest and differentiation of the melanocyte lineage. SOX10 is expressed during the specification of migrating neural crest cells and persists in neurons and melanocytes. During late-stage neural crest formation, SOX10 cooperates with other transcription factors of the SOXE family, forkhead box D3 (FOXD3), paired box gene 3 (PAX3), and activator protein 2 alpha (AP-2α) (Wahlbuhl et al., 2012). SOX10 plays a crucial part during differentiation of the melanocyte lineage because it directly regulates the expression of lineage-specific transcription factor MITF. By interacting with MITF it controls the expression of melanogenic enzymes, such as dopachrome tautomerase (DCT), tyrosinase (TYR), tyrosinase-related protein 1 (TYRP1). Consequently, diseases caused by SOX10 mutation (Waardenburg syndrome type 4C and 2E, central or peripheral demyelination, Hirschsprung disease) present with hypopigmentation and hearing loss (Pingault et al., 2022).

In addition to being a key player during embryonic development, SOX10 has been linked to initiation and maintenance of melanoma. SOX10 is expressed in most primary and metastatic melanoma cell lines (Flammiger et al., 2009).

1.7 Research questions

In summary, the CDM data suggests that there is a highly druggable cysteine residue, C71, located in the dimerization domain of SOX10. SOX10 is a lineage-specific transcription factor in melanoma. The following questions will be asked:

1) Do melanoma cell lines depend on SOX10 expression regarding their proliferation, i.e., do SOX10-expressing melanoma cell lines stop proliferating once depleted of the transcription factor?
2) How do SOX10 and MITF expression relate to one another? How do melanoma cell lines respond to MITF knockout?

Adduction by a covalent electrophilic inhibitor could provide an opportunity to target SOX10 offering a potential treatment strategy for melanoma patients. It will be inquired:

3) How can an electrophilic, cysteine-reactive covalent inhibitor that will engage with SOX10 be identified?

Underlying mechanisms will be investigated.

4) How can compounds be validated, and their mechanism of action be revealed?
5) How does the transcription factor function? What role does C71 play in SOX10 function?

2. Materials and methods

2.1 Experimental model details

All cell lines were either obtained from ATCC or a gift from Dr. Chris Ott (Massachusetts General Hospital)**.** All cells were maintained at 37 degrees Celsius with 5 % CO_2.
U257, U62, LOX-IMWI, G361, COLO792, COLO679, MEL-JUSO, IPC298, RVH-421, WM793B were cultured in Corning® RPMI 1640 1X medium (Fisher Scientific, 15-040-CV) supplemented with 10 % fetal bovine serum (Corning LifeSciences, 35-010-CV), 100 U/ml penicillin and 100 µg/ml streptomycin (Sigma, 15140122) and 1x Glutamax-I (Fisher Scientific).
HEK293T, A375, SK-MEL2, RPMI795, Mewo, IGR39, WM266-4, SK-MEL5, SK-MEL30, HMCB, SK-MEL3, Hs944T were grown in Dulbecco's Modified Eagle's Medium (DMEM) (Fisher Scientific) supplemented with 10 % fetal bovine serum (Corning LifeSciences, 35-010-CV), 100 U/ml penicillin and 100 µg/ml streptomycin (Sigma, 15140122) and 2 mM L-glutamine (Corning, 25-005-CI).
IGR-37, A2058, C32 and IGR-1 required DMEM/F12 medium (Fisher Scientific), supplemented with fetal bovine serum (Corning), 100 U/ml penicillin and 100 µg/ml streptomycin (Sigma).

2.2 Methods details

Cell Titer Glo Assay: 50 µl of Cell Titer Glo solution (Promega, G846) was added into each well, plate was covered in tin foil and incubated on shaker at room temperature (RT) for 10 min, luminescence was measured with a SpectraMax M5 plate reader (Molecular Devices) using an integration time of 500 ms. Wells were normalized to measurement on Day 0 (ratio of Day 6 / Day 0 raw value), then normalized to sgControl (or dimethyl sulfoxide (DMSO), depending on the experimental setup).

Cell (transient) transfection: Human SOX10 cDNA clone and the empty control vector pRK5 were purchased from Addgene. HEK293T cells were transiently transfected with

either the clone or pRK5 vector in the presence of 3 µl Polyethylenimine (Polysciences) / 1 µg plasmid DNA (ratio 3:1).

Co-immunoprecipitation experiments:

- Co-transfection: 2.5*10^6 cells were plated in 10 cm dishes. The next day, cells were transiently transfected with a total of 4 µg of pRK5-Flag-METAP2, pRK5-SOX10-Flag and pRK5-SOX10-HA in the following amounts in the presence of 12 µl Polyethylenimine (Polysciences): 2 µg of Flag-METAP/ SOX10-Flag + different amounts of SOX10-HA (100, 250, 500, 1000, 2000 ng) + respective amounts of pRK5 only (1900, 1750, 1500, 1000, 0 ng) were prepared in 500 µl of serum-free DMEM and added to the 10 cm dishes.
- (optional) Compound treatment in cells: 24 hours after transfection, media was aspirated and replaced by compound- or DMSO-containing media resulting in a final concentration of 20 µM. Treatment duration was either 3 or 6 hours.
- Protein lysis: If untreated, 24 hours after transfection, if treated, 3 or 6 hours after treatment, cells were scraped and lysed in 500 µl IP-base (40 mM HEPES (sigma, H3375) pH 7.4, 5mM MgCl2, 10 mM KCl) / 1 % Triton X-100 (sigma, T8787) + 1x EDTA-free protease inhibitor (sigma, 11873580001). Following lysis, samples were clarified by centrifugation for 10 min at 15,000 rpm. Protein concentration was determined by PierceTM BCA Protein Assay Kit (ThermoScientific, 23225) and 300 µg per each lysate in 500 µl IP-base / 1 % Triton prepared.
- FLAG-immunoprecipitations: Pulldown: Per sample, 30 µl Anti-FLAG M2 Affinity Gel (sigma, A2220, 50:50 slurry) were washed 4x with IP-base / 1 % Triton by centrifuging for 2 min at 6000 rpm each and added to the clarified supernatant and incubated for 3 h while rotating at 4 °C. Beads were centrifuged 1x at 6000 rpm for 2 min, washed 5x with IP-base/ 1 % Triton/ 150 mM NaCl by centrifuging for 1 min at 15,000 rpm each. 100 µl of beads were resuspended with equal amount of buffer and 30 µl of bead suspension (15 µl compact) were transferred into SOX10-HA lysates. 0/ 62.5/ 125/ 250/ 500 µg of SOX10-HA lysates were brought to 500 µl with IP-base / 1 % Triton. SOX10-HA was allowed to bind to immunoprecipitated Flag-tagged proteins for 3 h while rotating at 4 °C.
- 1x loading/sample buffer (50 µl) was added to the immunoprecipitated proteins which were subsequently denatured by boiling. Proteins were resolved by SDS-PAGE, then analyzed by immunoblotting.

Crystal Violet Assay: Culture media was aspirated off cells in 96-well plate, 50 µl Crystal Violet Solution (2.5 g crystal violet powder (ACROS) in 900 ml milli Q H2O + 100 ml Methanol, filtered) was added per well, incubated for 30 min, then washed 4 times with distilled water. Plates were allowed to dry overnight (at RT or at 37 °C), then quantified by image analysis. Plates were scanned using a table-top scanner as an 8-bit image at 600 dpi. Background was reduced and an unsharp mask applied. Data analysis was performed in FIJI / ImageJ. Threshold was set 0-100 using grayscale, each well was selected manually to measure that area. Integrated density was calculated = area * 1/mean (in a grayscale image, black receives a value of 0 and white = 255). Integrated density was then compared across conditions and expressed as % of control.

Hoechst 33342 staining for cell number quantification: Culture media was aspirated off 96-well plate, next, 1 µg/ml Hoechst 33342 (ThermoFisher) was added into each well. Wrapped in tin foil, plates were incubated for 30 min at RT on the shaker. Each well was then resuspended ten times, 80 µl were transferred into an opaque plate. Fluorescence was measured by the plate reader (excitation wavelength: 361 nm, emission wavelength: 486). “Buffer only” wells were subtracted from each well to calculate relative cell number. For each cell line, a standard curve was generated following measurement of fluorescence signal with 1000 / 2500 / 5000 / 7500 / 10,000 / 15,000 / 30,000 cells replated per well (n = 5).

In-vitro binding assay

- Confluent 10 cm dishes of transiently expressing FLAG-METAP2, SOX10-FLAG or SOX10-HA, respectively, were lysed with 1 ml IP-base (40 mM HEPES pH 7.4, 5 mM MgCl2, 10 mM KCl) / 1 % Triton X-100 (sigma) + 1x EDTA-free protease inhibitor (sigma). Following lysis, samples were clarified by centrifugation for 10 min at 15,000 rpm.
- For FLAG-immunoprecipitations, M2 Flag-agarose (200 µl, 50:50 slurry), washed with lysis buffer 1 % Triton / IP-base, were added to pre-cleared lysates of two 10 cm dishes of Flag-METAP2 / SOX10-Flag and incubated for 3 h by rotating at 4 °C.

- Following immunoprecipitation, the beads were washed with 1 % Triton / IP-base / 150 mM NaCl and were then added to respective SOX10-HA lysates for which the following protein amounts were determined by PierceTM BCA Protein Assay Kit (ThermoScientific, 23225): 0 / 62.5 / 125 / 250 / 500 / 1000 µg. 15 µl beads (compact) were transferred to each respective SOX10-HA lysate and incubated for 3 h while rotating at 4 °C. Following immunoprecipitation, the beads were washed with 1 % Triton / IP-base / 150 mM NaCl, 1x loading/sample buffer (50 µl) was added to the immunoprecipitated proteins which were subsequently denatured by boiling. Proteins were resolved by SDS-PAGE, analyzed by immunoblotting.

Library Screen

- SOX10 transcriptional reporter cells: I used U257 cells transduced with polyclonal pEZX-LvGA01-MITF-promoter-luciferase or TRPM1-promoter-luciferase. The cells were provided by Mariko Hara, PhD, Bar-Peled lab. The transgene was selected for using puromycin (sigma, at 0.67 µg/ml). The following MITF promoter (617 bp) was cloned into a pEZX vector (Genecopoeia):

CATCTATGTAGCTAAGAATAAGGTGCATATTAAGACCAGGATGCAAGAAGAGGCTGTT-
GAACTTGAACATTCAGCACAGAGTCTCTTCTCTTCTATACTAAAAGATAGTCATCCTGCAGTCGGAAGTG
GCAGTTATTCGGCCATTGGAAAAGTCTCATGTAATAGTAGCTTTTA-
GATGATGTCTCCTCCAAAGGGGCATTCTGCTATTAACCTATTGCTGAAAGAGAAATACCATTGTCTATTAA
TACTACTGGAACTAAAGATGAATAGTGAATTGGCCTTGATCTGACAGTGAGTTTGACTTTGA-
TAGCTCGTCACTTAAAAAGGTTCTTTTATATTTATGAAAAAAAGCATCACGTCAAGCCAGGGGGAAAAAT
TGATATCAACATTTAAGACCAAACTCGTAGGGCTTCCAAAAAAAAGGCCCTTATGTGAAC-
GTTTTTTTTTACATGCATAACTAATTAGCTTAGGTTATTATAAGCAGGGCTTCTGTGATAAAGTTTCCGGT
GGTGTCTCGGGATACCTTGTTTATAGTACCTTCTCTTTGCCAGTCCATCTTCAAATT-
GGAATTATAGAAAGTAGAGGGAGGGATAGTCTACCGTCTCTCACTGGATTGGTGCCACCTAAAACATTG

- Compound Treatment: Compounds were obtained from Enamine.
  U257 reporter cells were replated at 5000 cells / 100 µl / well in a 96-well plate. At 24 h after replating, cells were treated with library compounds at 5 / 2.5 µM (or DMSO). At 48 h after the compound treatment, the cells´ supernatant, containing secreted luciferase and alkaline phosphatase, was collected.

- Luciferase Assay: 10 µl supernatant was mixed with 50 µl of luciferase substrate (1x GL-H buffer, 1x GL-H reagent in autoclaved H_2O) and luminescence was measured using the plate reader (1500 ms). 20 µl of the supernatant was incubated with 80 µl of alkaline phosphatase substrate (1X Quanti-Blue Buffer, 1x QB reagent in autoclaved H_2O) at 37 °C until visible change of color. OD640 (absorbance) was then measured. All reagents belong to the Secrete-Pair Gaussia Luciferase assay Kit (Genecopoeia).
- Analysis: All results were normalized to DMSO (6 wells per plate). First, the average of all empty SEAP (secreted alkaline phosphatase) values was subtracted from all SEAP values, then normalized to DMSO. Raw luciferase values were divided by normalized SEAP values of corresponding wells, then normalized to DMSO.
- Selection of hits was based on the following criteria: Reduction of Gluc/SEAP by at least 30% (values <70, normalized to DMSO = 100) + 80 < SEAP < 120 + should not score in other screens (no reduction in other reporter cell lines by more than 30%), for example in an ovarian cancer cell line OVTOKO unrelated by biology.

Lentivirus production: HEK293T, cultured in DMEM / 10 % FBS / Pen / Strep / L-Glutamine, were plated on day 1 at 1.4*10^6 cells / 6 cm dish / 5 ml DMEM media and incubated at 37 °C for 18 to 24 h. On day 2, a packaging plasmid mixture (100 ng / µl) was prepared using 900 ng psPAX2 (envelope) and 100 ng VSV.G. 1 µg of sgRNA-encoding plasmids and 10 µl of packaging plasmid mixture (1 µg) were cotransfected using 6 µl of the X-TremeGENE HP transfection reagent. 3 µl / µg DNA (sigma) were added. 6 to 16 h after transfection, the media was changed to regular FBS-containing DMEM. Cells were kept in culture (> 48 h after transfection) and virus-containing supernatants were collected, then filtered using a syringe (0.45 µM filter), either used to infect target cells or stored at -20 °C.

Lentivirus infection (CRISPR-knockout) for melanoma cell lines: On day 1, cells were plated at 0.25 *10^6 cells / 1 ml / well in a 6-well plate for adherent cells. 1 ml of virus-containing supernatant, collected 48 h after transfection of HEK293T, was used to infect target cells in the presence of 1 µg / ml Polybrene Transfection Reagent (Sigma). Cells were incubated at 37 °C, media was changed at 24 h post-infection. Cells were allowed

to recover for an additional 24 h, then were trypsinized and replated on a 10 cm dish, including puromycin for selection, for subsequent experiments.

This method was provided by Mariko Hara, PhD, but is mentioned because the constructs generated by her were leveraged in succeeding experiments (growth assays). Lentiviral sgRNAs targeting the messenger RNA for human SOX10 and MITF were designed, amplified, and cloned into transient pLentiCRISPRv2 (addgene) vector at the restriction sites. The sequences for these sgRNAs are listed below (sequences are 5´ to 3´).

sgControl	caccGCCTGCCCTAAACCCCGGAA
sgSOX10_1	caccGGAGGAGCAGGACCTATCGG
sgSOX10_4	caccGGAGCAGGACCTATCGGAGG
sgMITF-6-fwd	caccgGATAGTCTACCGTCTCTCAC
sgMITF-6-rev	aaacGTGAGAGACGGTAGACTATCc
sgMITF-7-fwd	caccgCACCTAAAACATTGTTATGC
sgMITF-7-rev	aaacGCATAACAATGTTTTAGGTGc
sgMITF-8-fwd	caccgTCTACCGTCTCTCACTGGAT
sgMITF-8-rev	aaacATCCAGTGAGAGACGGTAGAc
sgMITF-9-fwd	caccgTTGCCAGTCCATCTTCAAAT
sgMITF-9-rev	aaacATTTGAAGATGGACTGGCAAc
sgMITF-10-fwd	caccgGGCACCAATCCAGTGAGAGA
sgMITF-10-rev	aaacTCTCTCACTGGATTGGTGCCc

Microscopy: Qualitative analysis by microscopic imaging. Representative pictures were taken with a Nikon Eclipse Ti 2 microscope, 10x magnification, gray scale.

Oligonucleotide pulldown assays

- Preparation of lysates:

1. U257: On day 1, 3*10^6 cells / 10 cm dish were replated. On day 2, dishes were lysed as described below.

2. HEK293T: On day 1, 2.5*10^6 cells / 10 cm dish were replated. On day 2, cells were transfected with 4 µg of plasmid DNA (pRK5-Flag-METAP2 / pRK5-SOX10(WT)-Flag / pRK5-SOX10(C71A)-Flag). 24 h after transfection, the cells were scraped. Cell pellets were lysed with 150 µl of 1 % NP-40 lysis buffer (50 mM Tris-HCl (pH 7.4), 150 mM NaCl, 1 % NP-40, 2 mM EDTA, 10 % Glycerol), then sonicated (amplitude 100 for 5 min).

· Annealing of oligonucleotides: IDT tubes were constituted with a TE buffer pH 8.0 (Invitrogen) at a final concentration of 100 µM. Next, 20 µl of forward and reverse oligonucleotides, respectively, were mixed and annealed using a thermocycler. The final concentration was adjusted to 1 µg / µl.
· DNA-agarose beads preincubation: Per sample, 30 µl of streptavidin agarose resin (Thermo Scientific) was washed with a DNA-binding buffer (DBB: 10 mM HEPES pH 7.4, 1 M NaCl, 10 mM EDTA, 0.05 % NP-40) three times by centrifugation by 2 min at 6000 rpm. After washing, the beads were resuspended in DBB, and 1 µg of oligo DNA / sample was added. Incubating the beads that were resuspended with DBB + DNA for 30 min to 2 h on a shaker at room temperature allowed for binding of DNA to those beads.
· Pull-down assay: Per sample, 400 µg of protein was used (protein concentration determined by BCA assay), diluted 1:10 with 50 mM Tris-HCl / 150 mM NaCl to get 0.1 % NP-40. Per sample, 10 µg poly (dI:dC) was added to capture non-specific DNA-binding proteins.
· Incubation of protein lysates with DNA-conjugated agarose: Following preincubation, the beads were washed twice with DBB, twice with a protein-binding buffer (PBB: 50 mM HEPES pH 7.4, 150 mM NaCl, 0.1 % NP-40) by centrifugation for 2 min at 6000 rpm, then resuspended with an appropriate amount of PBB to add 50 µl of bead suspension into each protein lysate. DNA-conjugated agarose beads were then incubated with protein lysates by a 3-hour or overnight rotation at 4 °C. After that, beads were washed with 500 µl PBB four times and any remaining buffer was removed using an insulin syringe. Next, 50 µl of 1x sample buffer (diluted 5x SB with 1 % NP-40 lysis buffer) were added into each sample and boiled at 95 °C for 5 min. The protein eluted from the beads were subjected to SDS-PAGE.

The following oligonucleotides were employed as described but initially designed by Mariko Hara, PhD.

MITF-promoter-WT-SOX10 binding site-fwd:
5´-bio-TAACCTATTGCTGAAAGAGAAATACCATTGTCTATTAA
MITF-promoter-WT-SOX10 binding site-rev:
5´-bio-TTAATAGACAATGGTATTTCTCTTTCAGCAATAGGTTAA
MITF-promoter-mut-SOX10 binding site-fwd:
5´-bio-TTAACCTAccGCTGAAAGAGAAATACCAccGTCTATTAA
MITF-promoter-mut-SOX10 binding site-rev:
5´-bio-TTAATAGACggTGGTATTTCTCTTTCAGCggTAGGTTAA
SoCM-probe-fwd: 5'-bio-AGACTGAGAACAAAGCGCTCTCACAC
SoCM-probe-rev: 5'-bio-GTGTGAGAGCGCTTTGTTCTCAGTCT
MIA-promoter-WT-fwd: 5'-bio-TGGTAATCAAAGGGCTGCCTTGTTCTCCTGC
MIA-promoter-WT-rev: 5'-bio-GCAGGAGAACAAGGCAGCCCTTTGATTACCA
MIA-promoter-mut-fwd: 5'-bio-TGGTAATCccAGGGCTGCCggtgTCTCCTGC
MIA-promoter-mut-rev: 5'-bio-GCAGGAGAcaccGGCAGCCCTggGATTACCA

Protein extraction: Cells were scraped into 1 ml of ice-cold PBS, spun down at 3500 rpm for 3 min at 4 °C. PBS was aspirated and cell pellet was lysed in 50 µl of 1 % NP-40 lysis buffer (50 mM Tris-HCl (pH 7.4), 150 mM NaCl, 1 % NP-40, 2 mM EDTA, 10 % Glycerol) + 1x EDTA-free protease inhibitor (sigma) + 1x benzonase (Santa Cruz Biotechnology. Samples were sonicated in a water bath sonicator at 4 °C, amplitude 100 for 5 min, then rotated end-over-end for 30 min at 4 °C. Lysates were clarified by centrifugation at 15,000 rpm for 10 min at 4 °C, supernatant was collected. Protein concentration was determined using BCA protein assay kit (Pierce), using BSA 0, 0.5, 1.0, 2.0 µg / µl as standards. Samples were normalized to 1 µg / µl, 5X loading dye was added. Samples were vortexed, spun down, boiled at 95 °C for 5 min, then loaded onto a gel.

Quantitative reverse-transcriptase (qRT)-PCR:
RNA extraction / cDNA synthesis / quantitative PCR analysis

- U257 was plated at 50,000 cells / well in a 12-well plate, U62 and SK-MEL28 were plated at 150,000 cells / well in 12-well plates. After 24h, cells were treated with 10 µM or DMSO for 48 hours.
- Total RNA was isolated using the Quick-RNA ™ MiniPrep Kit (Zymo Research) according to the manufacturer's protocol, except for one alteration: After the last wash using 400 µl RNA Wash Buffer, the empty columns were spun for 3 min (14,000 rpm) to completely dry out the membranes. RNA was eluted with 20 µl DNase / RNase-free water, incubated at RT for 1-2 min, then spun down again for 3 min (14,000 rpm).
- cDNA amplification was performed using iScript cDNA Synthesis Kit (Bio-Rad). qPCR primer sequences were obtained from Primer Bank (https://pga.mgh.harvard.edu/primerbank/) and are listed under “Key Resources”. qPCR analysis was performed using LightCycler 480 System (Roche) (95C, 15 sec + 60C, 60 sec) x 40 cycles, using “Abs Quant/2d Derivative Max for All Samples” with the SYBR green Mastermix (ThermoScientific).
- Normalization was executed on the housekeeping gene (β-actin) and calculated according to the ΔΔCt algorithm. Results are presented as fold expression of the control, one-fold reperesenting the same level of expression as the control. Forward (F) and reverse (R) primer names and their respective sequences for both housekeeping and SOX10 target genes are listed below.

housekeeping genes	
b-actin-F	TGAAGTGTGACGTGGACATC
b-actin-R	GGAGGAGCAATGATCTTGAT
SOX 10 target genes	
F1-hMITF	CCGTCTCTCACTGGATTGGT
R1-hMITF	TACTTGGTGGGGTTTTCGAG
F1-hSOX10	CCTCACAGATCGCCTACACC

R1-hSOX10	CATATAGGAGAAGGCCGAGTAGA
F1-ACSS1	GTGCAGAGTCCTTGGCTGGG
R1-ACSS1	TTCTTCAGCTCCACCACGCG
F1-IL16	GCCGAAGACCCTTGGGTTAG
R1-IL16	GCTGGCATTGGGCTGTAGA
F1-SGCD	GCGGAAACGATGCCTGTATTT
R1-SGCD	TGGCGTAGAGAGGTTGTAAGAA
F1-GAS7	CATCGCCAAGCAAAAAGCAGA
R1-GAS7	AGCCCAGAAGTAGTCGCAGT
F1-RNF144A	GAGCAGATGACAACCATAGCC
R1-RNF144A	TGCACTCAATCTCGTTCTCCT
F1-MIA	GGGCCAAGTGGTGTATGTCT
R1-MIA	CAGATCTCCATAGTAATCTCCCTGA
F1-RAB7A	GTGTTGCTGAAGGTTATCATCCT
R1-RAB7A	GCTCCTATTGTGGCTTTGTACTG
F1-HSPE1	ATGGCAGGACAAGCGTTTAGA
R1-HSPE1	CCGATCCAACAGCGACTACT
F1-RXRG	CCGGATCTCTGGTTAAACACATC
R1-RXRG	GTCCTTCCTTATCGTCCTCTTGA
F1-HSPD1	ATGCTTCGGTTACCCACAGTC
R1-HSPD1	AGCCCGAGTGAGATGAGGAG

siRNA transfection of melanoma reporter cell line: Cells were trypsinized, then 300,000 cells / 1.5 ml / well plated in 6-well plate. Two wells were plated per sample, one for immunoblotting, the other one was later trypsinized and replated on a 96-well plate to perform luciferase assay of the reporter cell line. Per well, 2 µl of 20 µM siRNA (siSOX10, siMITF – both obtained from Dharmacon, sequences listed below), 7.5 µl Lipofectamine RNAimax were added to 500 µl Opti-MEM (Life Technologies). Mix was resuspended and incubated for 15 min at RT for complex formation. This mixture was added to melanoma cells in 6-well plates with culture media to a final volume of 2.5 ml. At 24 h after transfection, the medium was changed. At 48 h after transfection, only one out of the duplicate wells was trypsinized and replated at 10,000 cells / well / 100 µl - 10 wells per each sample. At 72 h following transfection, the remaining cells in the 6-well plate were lysed for

Western Blot. Media was aspirated and changed into heat-inactivated FBS-containing RPMI for the 96-well plate wells. At 96 h after transfection, the supernatant of 96-well plates was collected to then perform luciferase assay.
The following siRNAs were employed in this assay, but initially designed by Mariko Hara, PhD.

siSOX10	Dharmacon	L-017192-00-0005, ON-TARGETplus Human SOX10 (SMARTpool 5nmol)
siMITF	Dharmacon	M-008674-00-0005, siGENOME Human MITF (SMARTpool 5 nmol)

Western Blot analysis: Protein samples (15-30 µg protein per lane) were loaded and separated on 10 % SDS-PAGE gels using a 1x running buffer (10x stock solution: 60 g Tris-base, 288 g glycine, 20 g SDS powder in 2 l miliQ water) at 200 V constant for 70 min, then transferred to an Immobilon-P Transfer Membrane (PVDF, Milipore, IPVH00010) which had been activated in 100 % methanol, then equilibrated on a shaker in 1x transfer buffer (1.8 l distilled H2O, 200 ml ethanol, 4.44 g CAPS (sigma, C2632-1KG), 10 NaOH pellets (ThermoFisher, S318-500)). Gel and PVDF membrane were sandwiched by two pieces of Fisherbrand™ Pure Cellulose Chromatography Papers, transferred at 250 mM constant for 2.5 h. Membrane was rinsed once in TBS / T, then blocked in 5 % skim milk / TBS-T for 30 min and incubated with primary antibody solution in 5 % BSA / TBS-T / sodium azide (sigma, 71289-5G) overnight. After washing the membranes three times for 5 min each in TBS-T, they were further incubated with secondary antibodies coupled to HRP for 1 h (1 % skim milk / TBS-T, anti-rabbit / anti-mouse 1:5000). After washing, the blot signals were visualized using Pierce™ ECL Western Blotting Substrate (ThermoScientific, 32106).

3 + 6 - day compound treatment in melanoma reporter cell line for proliferation assays: On day 0, 250,000 cells / 2 ml / well were replated in a 6-well plate. Cells were treated with 2 ml of compound-containing media at 5 / 2.5 µM / DMSO, then left in culture for 3 days. On day 3, cells were trypsinized and replated on two 96-well plates (10 wells each), using the cell number / 50 µl / well previously optimized and used in sgSOX10 growth assays. Cells were then treated with 50 µl of compound-containing media at 5 / 2.5 µM / DMSO and left in culture for 6 days. On day 9, one plate was used for crystal violet staining

and subsequent image analysis (as described above), the other one was stained with Hoechst dye.

Statistical analysis: Statistical analyses were performed using GraphPad Prism 9 (GraphPad Software, Inc.). Different sample sizes (n) were chosen for different cell lines as mentioned in the respective description. All results are presented as means ± standard deviation. Significance levels between groups were determined using two-way analysis of variance (ANOVA) with Tukey´s post hoc test. When calculating statistical significance to a p-value < 0.05, the statistical significance is illustrated by *, whereas ** represents p < 0.01, *** represents p < 0.001, and **** represents p < 0.0001.

Graphical representation: Figures were prepared using GraphPad Prism 9 (GraphPad Software, Inc.)

2.3 Key resources table

Table 1: Antibodies

Reagent	Source	Identifier
beta(ß)-actin (13E5) rabbit mAb	CST	4970S
DYKDDDDK Tag (D6W5B), rabbit mAb	CST	14793L
GAPDH antibody, Mouse mAb	Sigma	G8795
HA-Tag (C29F4) Rabbit mAb	CST	3724S
Lamin A/C (4C11) Mouse mAb	CST	4777S
MITF (D5G7V) Rabbit mAb	CST	12590S
Raptor (24C12) Rabbit mAb	CST	2280s
SOX10 (D5V9L) rabbit mAb	CST	89356T
HRP-labelled anti-rabbit IgG	CST	7074s
HRP-labelled anti-mouse IgG	CST	7076s

Table 2: Chemicals, peptides, and recombinant proteins

Reagent	Source	Identifier
Anti-FLAG M2 Affinity Gel	Sigma	LOT# SLCH0130
Benzonase® nuclease lyophilized powder, 50 KU	Santa Cruz Biotechnology	Sc-391121B-50KU
BMOE (bismaleimidoethane)	ThermoFisher	22323
BMH (bismaleimidohexane)	ThermoFisher	22330
CellTiter-GloR One Solution Assay	Promega	G8462, LOT 0000380035
Crystal Violet, certified	ACROS	40583-0250, CAS:548-62-9
cOmplete™, EDTA-free Protease Inhibitor Cocktail	Sigma-Aldrich	11873580001
DTT, molecular biology grade (dithiothreitol, Cleland`s reagent)	ThermoScientific	01091645
DMSO Corning™ (Dimethyl Sulfoxide)	Fisher	MT25950CQC
Hoechst 33342	ThermoFisher	H1399
LightShift TM Poly (dI:dC)	ThermoFisher	Lot# WK334837
Lipofectamine RNAiMAX Transfection Reagent	ThermoFisher	13778150
Opti-MEM™ I	ThermoFisher	11058021
Polybrene Infection / Transfection Reagent	Sigma Aldrich	TR-1003-G
Polyethylenimine, linear, MW 25000, Transfection Grade (PEI 25K TM)	Polysciences	23966-100
Poly-L-lysine solution	Sigma Aldrich	P8920-100ML
Puromycin	Sigma	P8833-100MG
Streptavidin agarose resin	ThermoFisher	5 ml
SYBR™ Green PCR Master Mix	ThermoFisher	4312704
TE Buffer, pH 8.0, RNase Free	Invitrogen	AM9849
X-tremeGENE™ HP DNA Transfection Reagent	Millipore	6366236001

Table 3: Critical commercial assays

Reagent	Source	Identifier
PierceTM BCA Protein Assay Kit	ThermoScientific	23225
Zymo Research Kit Quick-RNA™ MiniPrep (50)	Genesee scientific	11-327
SYBR Green Master Mix	Applied Biosystems	4309155
iScript cDNA Synthesis Kit 100 rxns.	Bio-Rad	1708891
Secrete-Pair Gaussia Luciferase assay Kit (1000 rxns, LF062)	Genecopoeia	LF062

3. Results

3.1 Deciphering the biological role of transcription factor SOX10 in melanoma cell lines

SOX10 is expressed in most primary and metastatic melanoma cell lines. Herein, I depleted 26 melanoma cell lines of the transcription factor by sgRNA-guided knockout. Successful SOX10 knockout was first confirmed by immunoblot, for example in SK-MEL5. In addition, protein levels of MITF which is a main target gene of SOX10 were visibly decreased following knockout of SOX10, too **(Figure 3a)**.

Transduced cells were then assessed for changes in cell proliferation. Growth assays such as cell titer glo assay – generating a readout of ATP levels via luminescence – or crystal violet assay – staining for DNA content – followed by image analysis in ImageJ, allowed for quantitative measurements of potential proliferation defects. Regarding SK-MEL5, cell titer glo assay results revealed a significant decrease in cell growth by 72.6 % or 69.6 % for cells transduced with sgSOX10_1 or sgSOX10_4, respectively **(Figure 3b)** **(**$p < 0.0001$**).** Microscopy pictures taken with 10x magnification reflected the loss of cell viability quantified: Cell density was visibly reduced, and cell bodies were elongated, flat and translucent **(Figure 3c)**. Taken together, SK-MEL5 showed a significant reduction in cell viability using both cell titer glo and crystal violet assay, suggesting a critical role for SOX10 in melanoma cell survival.

These inhibition studies were then performed in 26 melanoma cell lines and revealed a significant impairment of cell proliferation, as measured by cell titer glo assay, for most melanoma cell lines, whereas only a minority remained unaffected or even increased their proliferation following SOX10 depletion **(Figure 4a)**. Next, immunoblotting protein samples of the 26 melanoma cell lines investigated allow to compare SOX10 protein levels with a decrease in cell proliferation in the respective cell line **(Figure 4b)**.

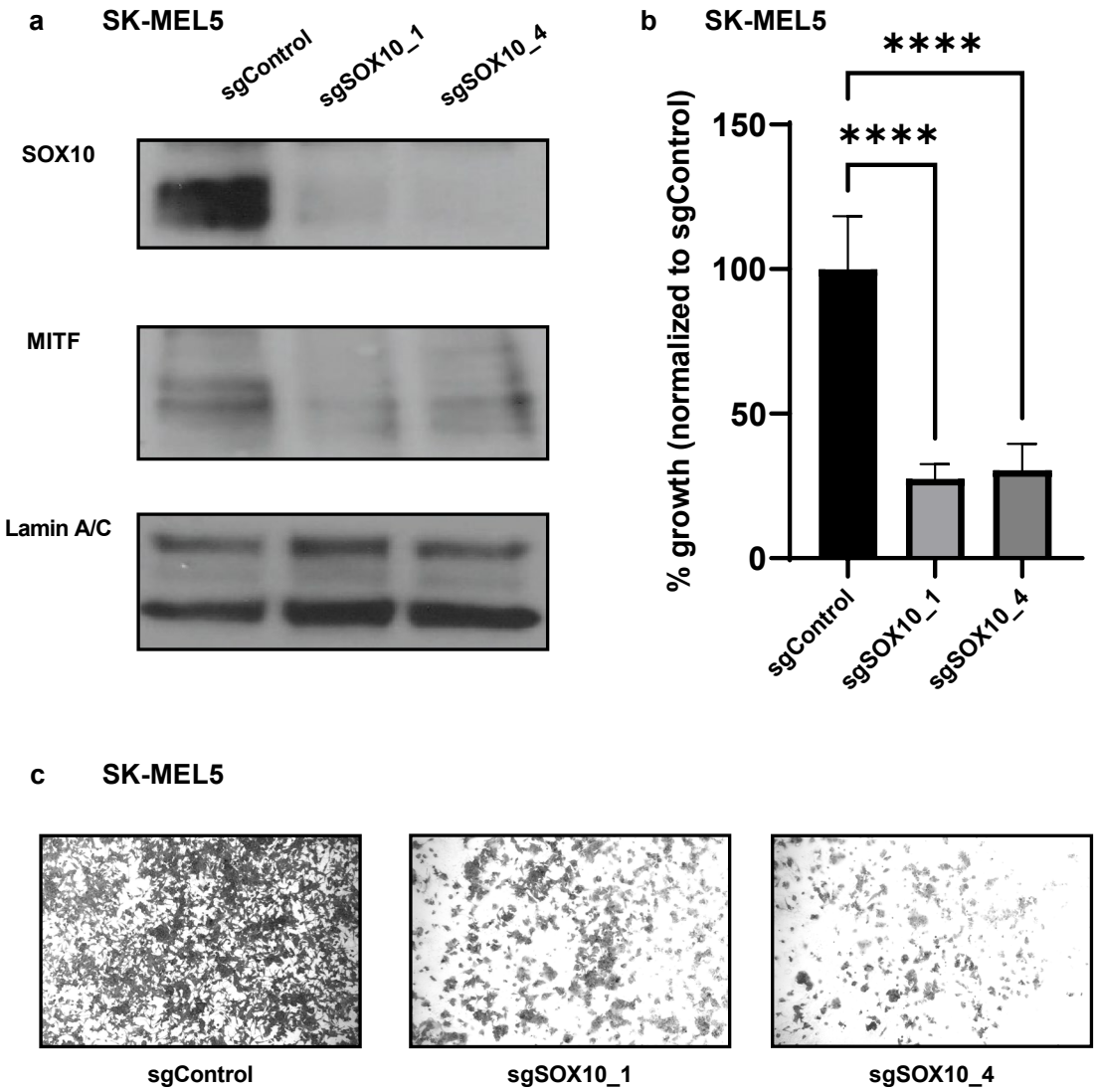

Figure 3: SOX10 regulates melanoma proliferation
a, Western Blot analysis of SOX10 and MITF levels in SK-MEL5 cells targeted by two independent sgRNA vectors. SgSOX10_1 and sgSOX10_4 were individually introduced into SK-MEL5 cells by lentiviral transduction. Lamin A/C served as loading control.
b, Growth assay of SOX10-depleted SK-MEL5. Cells were transduced with lentiviral sgSOX10_1, sgSOX10_4, or sgControl, followed by puromycin selection. Cells were cultured with puromycin for 6 days and cell viability was determined by cell titer glo assay according to the manufacturer's instruction. The results are presented as mean ± standard deviation of measurement replicates, n = 10. Significance levels were determined using two-way ANOVA with Tukey´s post hoc test (*p<0.05, **p<0.01, ***p<0.001, ****p<0.0001)
c, Crystal violet imaging of SK-MEL5 transduced with lentiviral sgSOX10_1, sgSOX10_4, or sgControl. Cells were cultured with puromycin for 6 days and stained with Crystal Violet. Pictures were taken with a Nikon Eclipse Ti 2 microscope, 10x magnification.

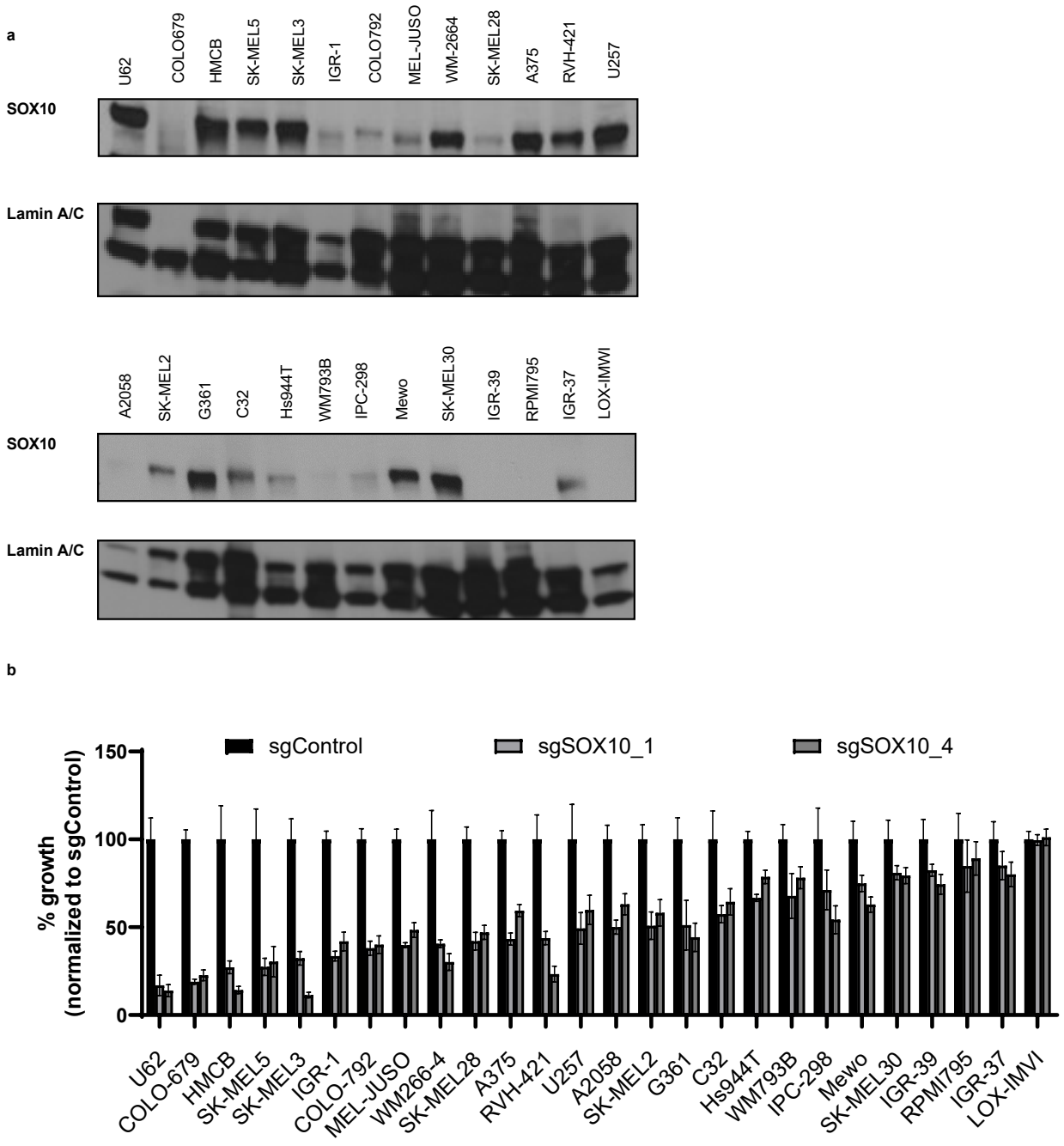

Figure 4: Correlation between SOX10 protein level and growth impairment following SOX10 depletion

a, Western Blot analysis of SOX10 protein levels across melanoma cell lines (molecular weight of SOX10 ~60 kDa). Lamin A/C served as loading control. **b,** Growth assay of SOX10-depleted melanoma cell lines, order based on % growth reduction in sgSOX10_1. Cells were transduced with lentiviral sgSOX10_1, sgSOX10_4, or sgControl, followed by puromycin selection. Cells were cultured with puromycin for 6 days and cell viability was determined by Cell Titer Glo assay according to the manufacturer's instruction. Except for LOX-IMWI, all the reduction in % growth is significant for both sgSOX10 _1 and

sgSOX10_4. The results are presented as mean ± standard deviation of measurement replicates, n = 10.

Next, MITF levels were examined. U257 and A375 were chosen as experimental models because they had been described as SOX10-positive / MITF-high level and SOX10-positive / MITF-low level, respectively. In a similar manner to the SOX10 depletion experiments described above, proliferation in both cell lines was evaluated following sgRNA-guided knockout of MITF. As expected, depletion of MITF in high-MITF expressing U257 via three different single guide RNAs led to a significant decrease in cell viability (sgMITF_6 $p < 0.001$, sgMITF_10 $p < 0.01$), whereas the A375 cells, expressing MITF to a lesser extent, did not respond to the knockout **(Figure 5a, b)**.

3.2 Identifying a cysteine-reactive small-molecule compound that decreases SOX10 transcriptional activity

Cysteine druggability mapping data had previously identified cysteine residue C71 as highly druggable and localized it to the dimerization domain of SOX10. Therefore, I aimed to identify an electrophilic small-molecule inhibitor able to target that cysteine residue and potentially disrupt SOX10 function.

There are several biochemical tools to study a transcription factor´s function, some of which were employed later in the project. However, to perform a large-scale compound screen – encompassing 1000+ electrophilic, cysteine-reactive, acrylamide small molecules – a high-throughput system had to be established. This is why a secreted luciferase-based reporter system was chosen. The reporter system measured SOX10 transcriptional activity by reading out activation of the MITF promoter as MITF is SOX10´s main target gene. The 613-bp promoter cloned into the luciferase vector comprised 7-8 putative SOX10 binding sites.

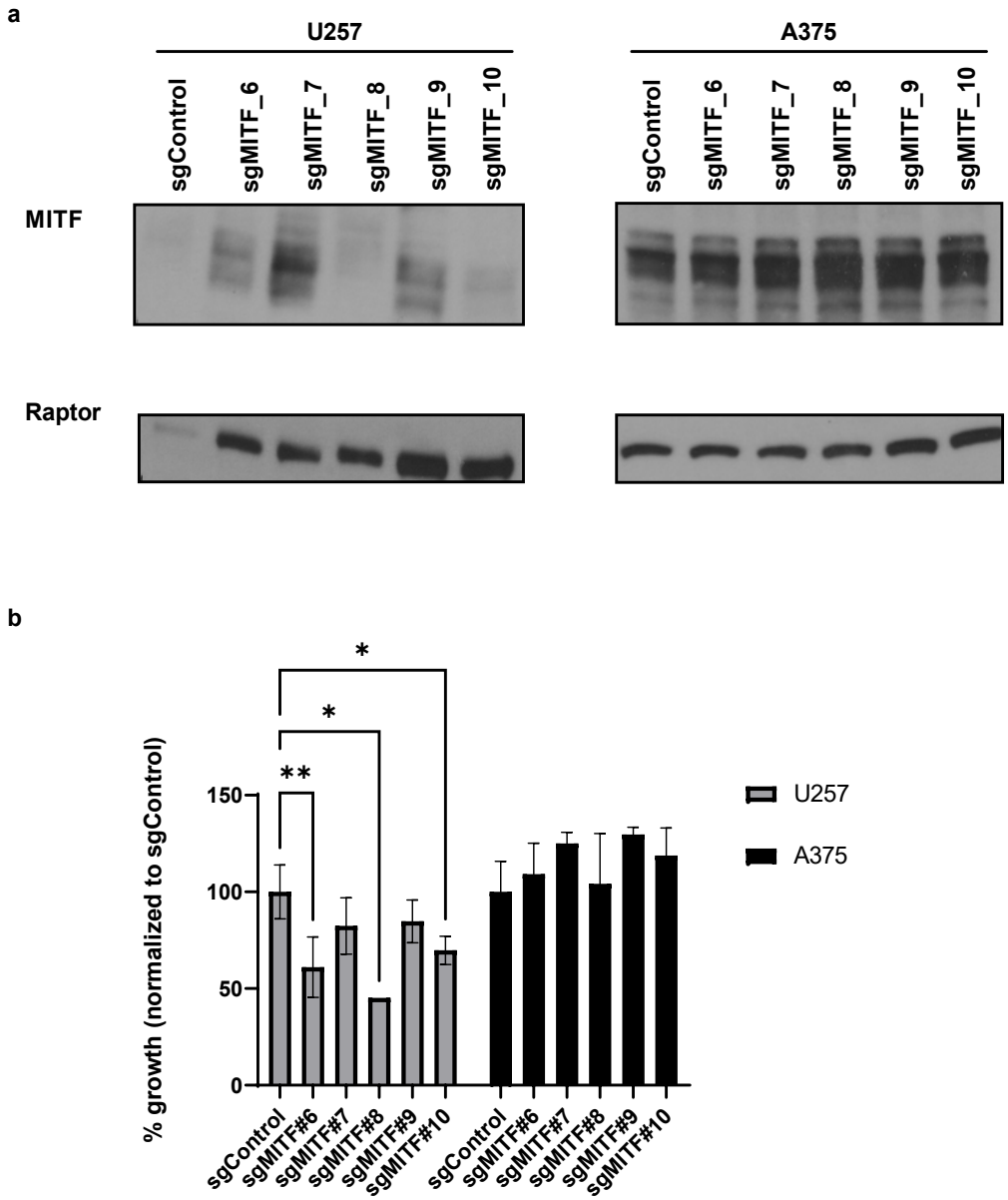

Figure 5: Correlation between MITF protein level and growth impairment following MITF depletion

a, Western Blot analysis of MITF levels in U257 (MITF-high) versus A375 (MITF-low) cells targeted by five independent sgRNA vectors. sgMITF_5 - 10 were individually introduced into U257 / A375 cells by lentiviral transduction. SgRNA-transduced cells were selected with puromycin (0.67 µg / ml) for 3 days, then replated at 75,000 cells / well in 6-well plates, selected for another 6 days, then lysed. Raptor served as loading control. **b,** Growth assay of MITF-depleted U257 and A375 shows significantly reduced cell proliferation in U257 cells only. Cell viability was determined by Crystal Violet assay (50 µl crystal violet solution per well). sgRNA-transduced A375 (1000 cells / well) vs. U257 (2500 cells / well) were replated in 96-well plates. The results are presented as mean ± standard deviation of measurement replicates, n = 5. Significance levels were determined using two-way ANOVA with Tukey´s post hoc test (*p<0.05, *p<0.01, ***p<0.001, ****p< 0.0001),

To set up the reporter assay, first, SOX10+ MITF-high melanoma cell line U257 was selected as most preliminary experiments had been performed in that cell line.

Second, U257 was transduced with either one of two following plasmids. To generate a “SOX10 reporter”, U257 was transduced with a plasmid that put luciferase expression under the control of MITF promoter and, as internal control, secreted embryonic alkaline phosphatase expression (SEAP) under the control of SV40 promoter.

In “MITF reporter” U257, luciferase expression was under the control of Transient receptor potential cation channel subfamily M member 1 (TRPM1) promoter with the same internal control. The TRPM1 promoter contains multiple MITF consensus binding elements as shown by chromatin immunoprecipitation of endogenous MITF within melanoma cells. What is more, according to clinical studies TRPM1 expression strongly predicts non-metastatic propensity and therefore correlates with a positive outcome (Miller et al., 2004).

Using SEAP driven by an SV40 constitutive promoter allowed to normalize cell viability and technical variations a high-throughput format might be susceptible to. Both reporter cell lines contained puromycin-resistant genes so that the transgene could be selected for using puromycin.

Lastly, the reporter systems were validated by knockdown using siRNA transfection. In siSOX10 and siMITF-treated cells, a decrease in SOX10 or MITF transcriptional activity was confirmed, as well as a decrease in the respective protein level by immunoblot **(Figure 6a)**.

All 1000+ library compounds contained an acrylamide moiety, a known warhead in drug discovery. Preliminary experiments performed in the reporter system had revealed a promising compound called “EAWU1”. EAWU1 was used to optimize screening conditions, i.e. treatment interval and cell number per well. A 48-hour treatment interval and plating 5000 cells / well in a 96-well format were determined the most effectful combination, achieving a decrease of SOX10 transcriptional activity by 50 % (Gluc / SEAP normalized to DMSO). Throughout the screen, EAWU1 served as positive control.

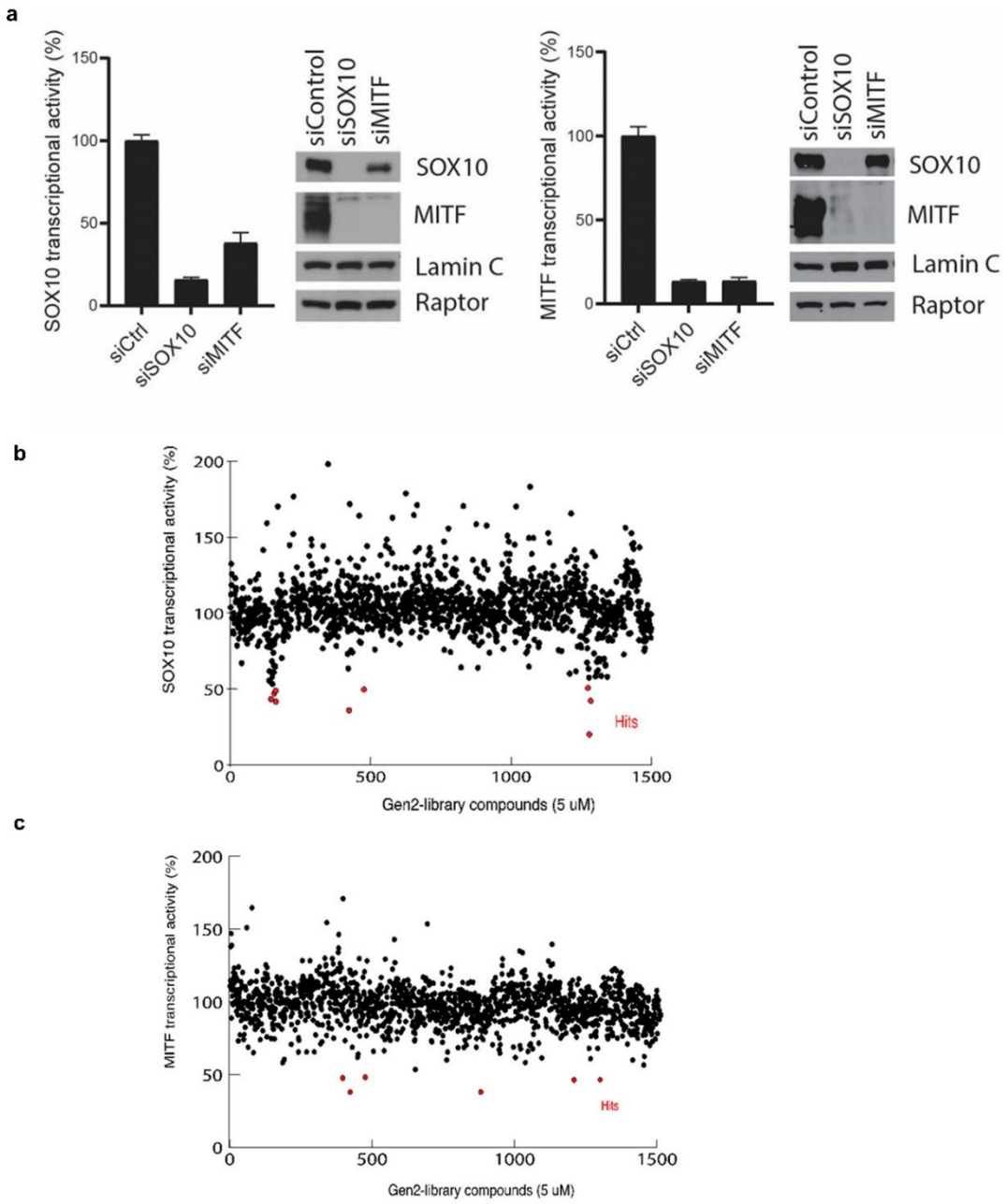

Figure 6: A small-molecule screen in luciferase-based SOX10/MITF-reporter system identifies promising covalent inhibitors

a, left – SOX10 transcriptional activity and immunoblot analysis in U257 SOX10 reporter cells transfected with indicated siRNA, **right –** MITF transcriptional activity and immunoblot analysis in U257 MITF reporter cells transfected with each indicated siRNA. The results are presented as mean ± standard deviation of measurement replicates, n = 10. **b,** Covalent inhibitor screen identifies compounds that, at a concentration of 5 µM, block SOX10 activity in U257 SOX10 reporter and **c,** MITF activity in U257 MITF reporter. % SOX10 or r. % SOX10 or MITF transcriptional activity was determined by secreted luciferase assay and is expressed as Gluc / SEAP: Raw Gaussia luciferase values (Gluc) divided by secreted embryonic alkaline phosphatase (SEAP) levels, then normalized to DMSO.

After establishing a valid SOX10 and MITF reporter system, cells were treated with 1000+ electrophilic, covalent, cysteine-reactive small-molecule compounds at 5 and 2.5 µM **(Figure 6b, c)**. Selection criteria defining “hit compounds” for follow-up experiments were, first, a reduction by 30 % in Gluc / SEAP (normalized to DMSO treatment) and, second, 80 % < SEAP < 120 % (normalized to DMSO).

MITF transcriptional activity was determined by secreted luciferase assay and is expressed as Gluc / SEAP: Raw Gaussia luciferase values (Gluc) divided by secreted embryonic alkaline phosphatase (SEAP) levels, then normalized to DMSO.

All hit compounds meeting named selection criteria were first validated in follow-up experiments, identifying compound 2-A01 as top hit compound. 2-A01, a benzanilide acrylamide **(Figure 7b, top)**, yielded a significant decrease in SOX10 transcriptional activity of about 78.4 % at 5 µM.

Next, studying structural analogs of 2-A01 allowed to identify additional compounds with increased potency such as compound SH-0029. SH-0029, a benzamide-THQ acrylamide **(Figure 7b, middle)**, showed a significant decrease in both SOX10 and MITF transcriptional activity (each $p < 0.0001$) at low micromolar concentrations and dose-dependent activity **(Figure 7a, left)**.

Furthermore, the search for overlap in chemical structure also revealed compound SH-0105 (**Figure 7b, bottom**) which showed no significant effect on transcriptional activity across a broad range of compound concentrations (20 / 10 / 5 / 2.5 µM) **(Figure 7a, right)**. This is why SH-0105 served as control compound in following experiments, replacing DMSO.

Finally, additional SOX10-dependent melanoma reporter cell lines, such as SK-MEL28 SOX10-reporter, U62 SOX10-reporter, A375 SOX10-reporter as well as G361 MITF reporter, were treated with SH-0029 (20 µM / 10 µM / 5 µM / 2.5 µM / vehicle) which yielded results comparable to the treatment in U257 reporters **(Figure 7c)**.

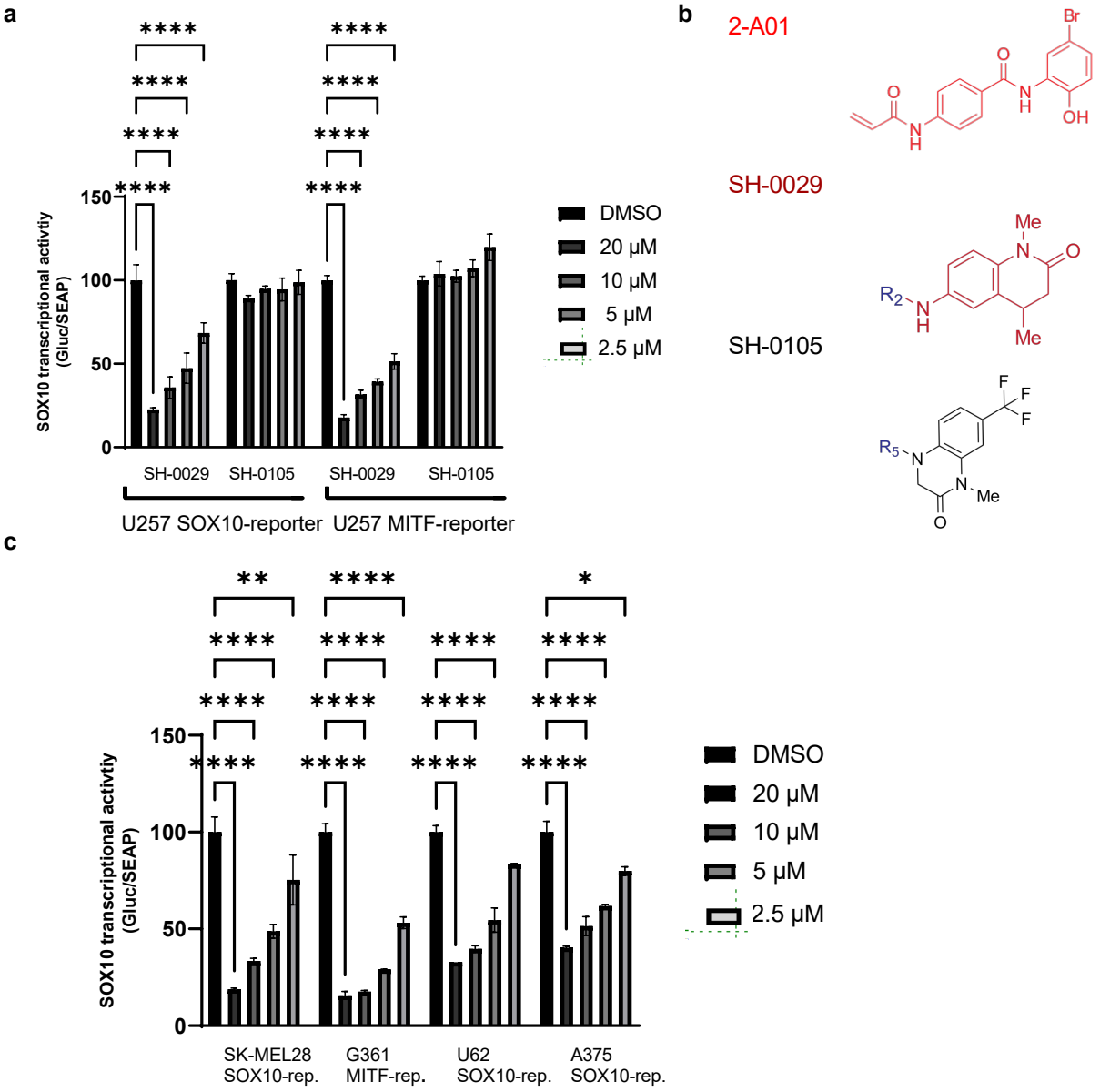

Figure 7: Hit compound SH-0029 impairs SOX10 transcriptional activity at low micromolar concentration.

a, Compound SH-0029 significantly decreases SOX10 transcriptional activity, whereas SH-0105 shows no effect. SOX10 transcriptional activity was determined by secreted luciferase assay and is expressed as Gluc / SEAP: Raw Gaussia luciferase values (Gluc) divided by secreted embryonic alkaline phosphatase (SEAP) levels, then normalized to DMSO. 5000 cells/well in a 96-well plate, treated with 20/10/5/2.5 µM of compound or DMSO for 48 h. **b,** Chemical structures of acrylamide small-molecules SH-0029, a benzamide-THQ acrylamide; 2-A01, a benzamide-THQ acrylamide; and acrylamide SH-0105. SH-0105 does not show any effect but has a similar chemical structure which makes it a suitable control compound. **c,** Hit compound SH-0029 shows similar effect in other SOX10-dependent, melanoma cell line reporters: SK-MEL28 SOX10-reporter, G361 MITF-reporter, U62 SOX10-reporter, A375 SOX10-reporter. 5000 cells / wells. All results

are presented as mean ± standard deviation of measurement replicates, n = 2. Significance levels were determined using two-way ANOVA with Tukey´s post hoc test (*p<0.05, **p<0.01, ***p<0.001, ****p<0.0001),

To verify that SH-0029 specifically targets SOX10, next, qPCR was performed. Primers for the following SOX10 target genes were chosen based on recent literature: First, MITF and melanoma inhibitory activity (MIA), both of which are regulated by SOX10 dimer. Second, Ras-associated protein 7A (RAB7A), heat shock proteins family D member 1 and family E member 1 (HSPD1 and HSPE1), all of which are shared target genes of SOX10 and Myc. Lastly, gene expression of retinoid x receptor gamma (RXRG), growth-arrest specific protein 7 (GAS7), ring finger protein 144A (RNF144A) was analyzed.

Depletion of SOX10 by siRNA-transfection in U257 confirmed that the expression of most of the genes selected was under the control of SOX10, as measured by the log2-fold change in siSOX10 versus siControl. SH-0029 treatment at 10 µM in U257, SK-MEL28 and U62 showed downregulation of SOX10 regulated genes to a comparable level of that induced by genetic ablation. These qPCR results indicated that SH-0029 treatment induces a gene signature specific to SOX10 **(Figure 8)**.

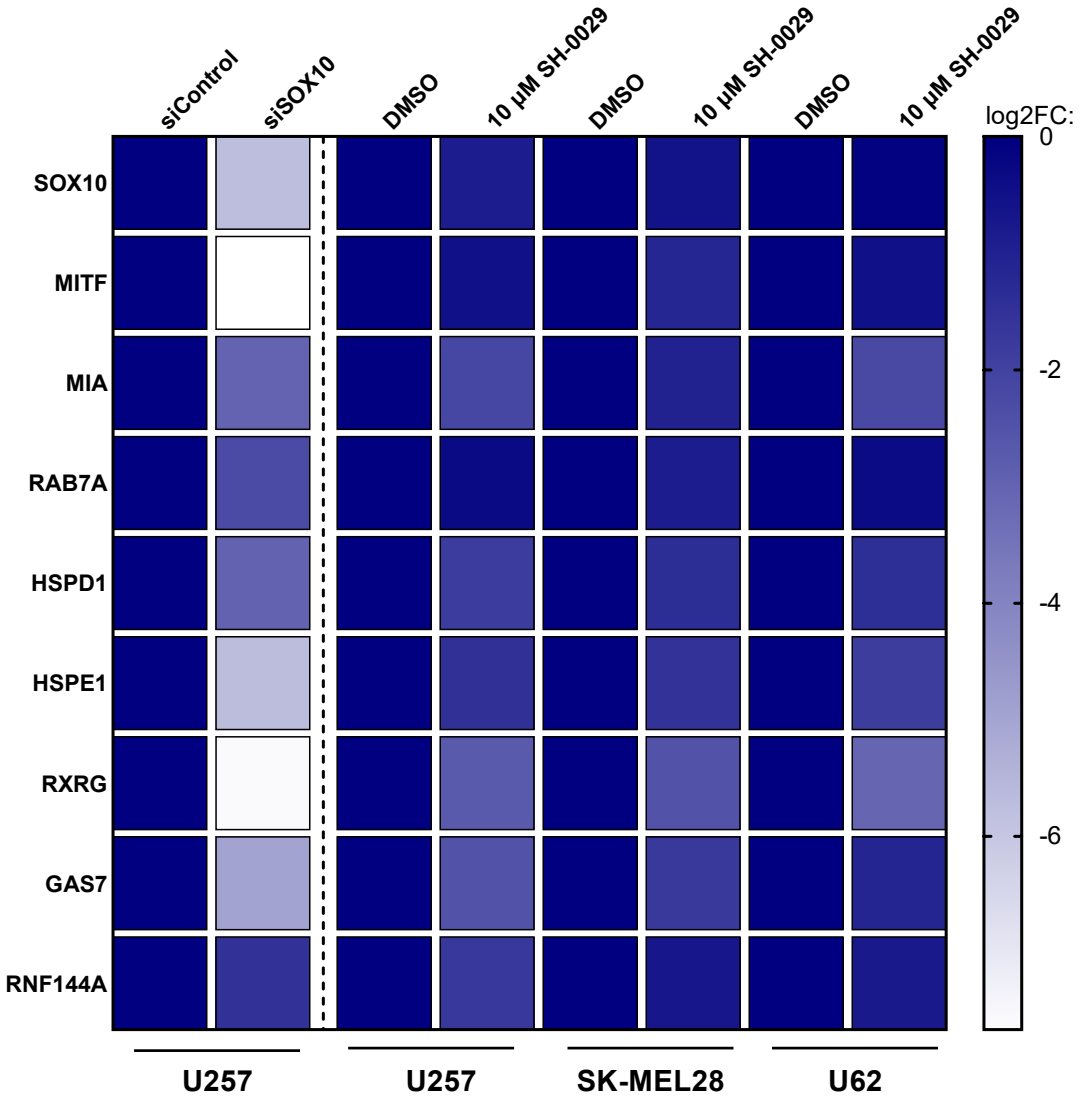

Figure 8: Quantitative PCR analysis of SOX10 regulated genes following compound treatment.
qPCR analysis of SOX10 regulated genes. Heatmap depicts log2 fold changes in relative gene expression. **Left** – U257 cells were transfected with siSOX10 or siControl and RNA was extracted at 72 h after transfection. **Right** – for compound treatment, U257 was re-plated at 50,000, U62 and SK-MEL28 at 150,000 cells / well per well in 12 well-plates and treated with the hit compound SH-0029 at 10 µM for 48 h. The results are presented as mean ± standard deviation of measurement replicates, n = 2 biological replicates and n = 3 technical replicates each. Significance levels are not depicted here.

3.3 Elucidating the compound´s mechanism of action

Preliminary experiments had localized ligandable C71 to SOX10´s dimerization domain. Therefore, it was hypothesized that C71 might be involved in SOX10 multimerization, and liganding by hit compound SH-0029 of C71 would affect this mechanism. To investigate underlying mechanisms, further functional assays were employed.

3.3.1 Protein-protein interaction assays

To assess protein-protein interaction of SOX10, co-immunoprecipitation assays using FLAG-tagged agarose were performed. FLAG- and HA-tagged SOX10 were co-transfected into HEK293T. By precipitating all FLAG-tagged protein using agarose beads, any protein bound to it could be revealed. Through its HA-tag, SOX10 could easily be identified among all proteins bound to FLAG-tagged and immunoprecipitated protein. Initially, 2000 ng of either SOX10-FLAG or, as control, FLAG-METAP2 were transfected into HEK293T, along with varying amounts of SOX10-HA and respective amounts of empty pRK5 vector. Titrating the transfected amount of SOX10-HA, i.e. 100, 200, 500, 1000 or 2000 ng allowed to identify the cut-off between specific and non-specific binding: 2000 ng of SOX-HA exhibited binding to both SOX10-FLAG and control protein FLAG-METAP2, suggesting nonspecific interaction. 1000 and 500 ng of SOX10-HA, however, showed a strong binding to SOX10-FLAG only and were therefore used in succeeding experiments **(Figure 9a)**. Next, co-transfected HEK293T cells were treated with SH-0029 or DMSO, respectively, for three hours, then subjected to immunoprecipitation as described. With both 500 and 1000 ng SOX10-HA transfected, 20 µM SH-0029 increased protein-protein binding compared to DMSO treatment (**Figure 9b**). To summarize, co-immunoprecipitation assays in HEK293T cells showed increased multimerization upon SH-0029 treatment.

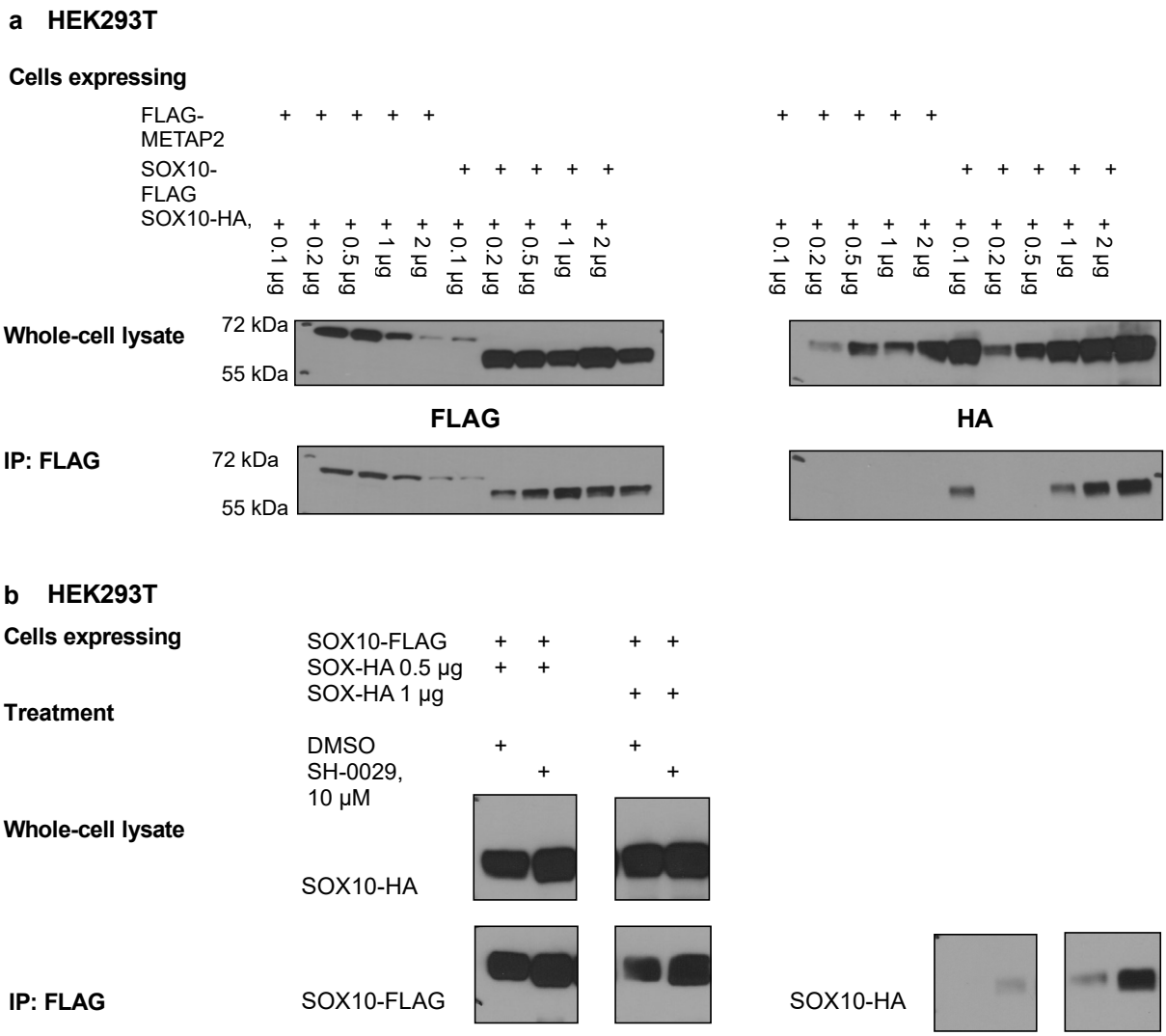

Figure 9: Protein-protein interaction assays
a, HEK293T was transiently co-transfected with FLAG-METAP2 or SOX10-FLAG, each plus titrated amounts of SOX10-HA. FLAG-immunoprecipitation of respective lysates was performed for 3 hours using 30 µl Anti-FLAG M2 affinity gel (50:50 slurry), bound protein was then eluted with 1x loading buffer. 500 / 1000 ng SOX10-HA co-immunoprecipitated with SOX10-Flag but not with control protein FLAG-METAP2 and were therefore chosen for subsequent experiments. **b,** Co-transfection of pRK5 SOX10-FLAG (2000 ng) with pRK5-SOX10-HA (500 or 1000 ng) into HEK293T. Transfected cells were treated with 20 µM SH-0029 for three hours, then subjected to cell lysis, followed by co-immunoprecipitation. α-FLAG and α-HA, 1:1000, CST.

3.3.2 Protein-DNA interaction assays

Considering qPCR and co-immunoprecipitation results of SH-0029 treatment, it was hypothesized that increased interaction of SOX10 with SOX10, or potential additional interaction partners, impairs SOX10 signaling. It was therefore asked how the increased multimerization of SOX10 elicited by SH-0029 led to downregulation of SOX10 transcriptional signaling.

To that end, interaction of SOX10 and target DNA was investigated by oligonucleotide pulldown assays. This approach uses small DNA fragments, i.e., 8 to 50 nucleotides in length. For SOX10, MITF was favored as target gene in this experiment because their relation has been studied extensively. In this assay, out of the MITF promoter used in the luciferase reporter assay which is 613 bp in length and contains 7 putative SOX10 binding sites, a 40-base-pair (bp) section was selected comprising SOX10 binding site 4 and 5, then biotinylated.

First, in U257 lysate the binding of SOX10 to the wild type oligonucleotide MITF promoter (40 bp) was confirmed. No SOX10 protein was found bound to the mutated oligonucleotide MITF promotor (40 bp). In accordance with common practice, a synthetic, non-biotinylated competitor polymer (poly dI-dC) was added to the reaction mixture to capture non-specific DNA binding proteins **(Figure 10a, left)** (Larouche et al., 1996). Additionally, an oligonucleotide containing the SOX family consensus motif = SoCM (total 26 bp) was generated. Similarly, SOX10 demonstrated binding to the SOX family consensus motif oligonucleotide and wildtype MIA oligonucleotide but failed to interact with a mutated MIA oligonucleotide **(Figure 10a, right)**. Next, SOX10(WT)-FLAG and SOX10(C71A) were transfected into HEK293T and whole-cell lysate FLAG and SOX10 levels confirmed by immunoblot. The respective lysates were then incubated with streptavidin beads containing the biotinylated wildtype MITF promotor. It was shown that wildtype SOX10 was able to bind wildtype MITF promotor similarly to binding of endogenous SOX10 in U257. C71-mutated SOX10 expressed in HEK293T cells, however, showed markedly reduced binding towildtype promotor **(Figure 10b, left)**. When analyzing interaction of SOX10, both wild type and mutated, with SoCM promotor, no difference was detected (**Figure 10b, right**).

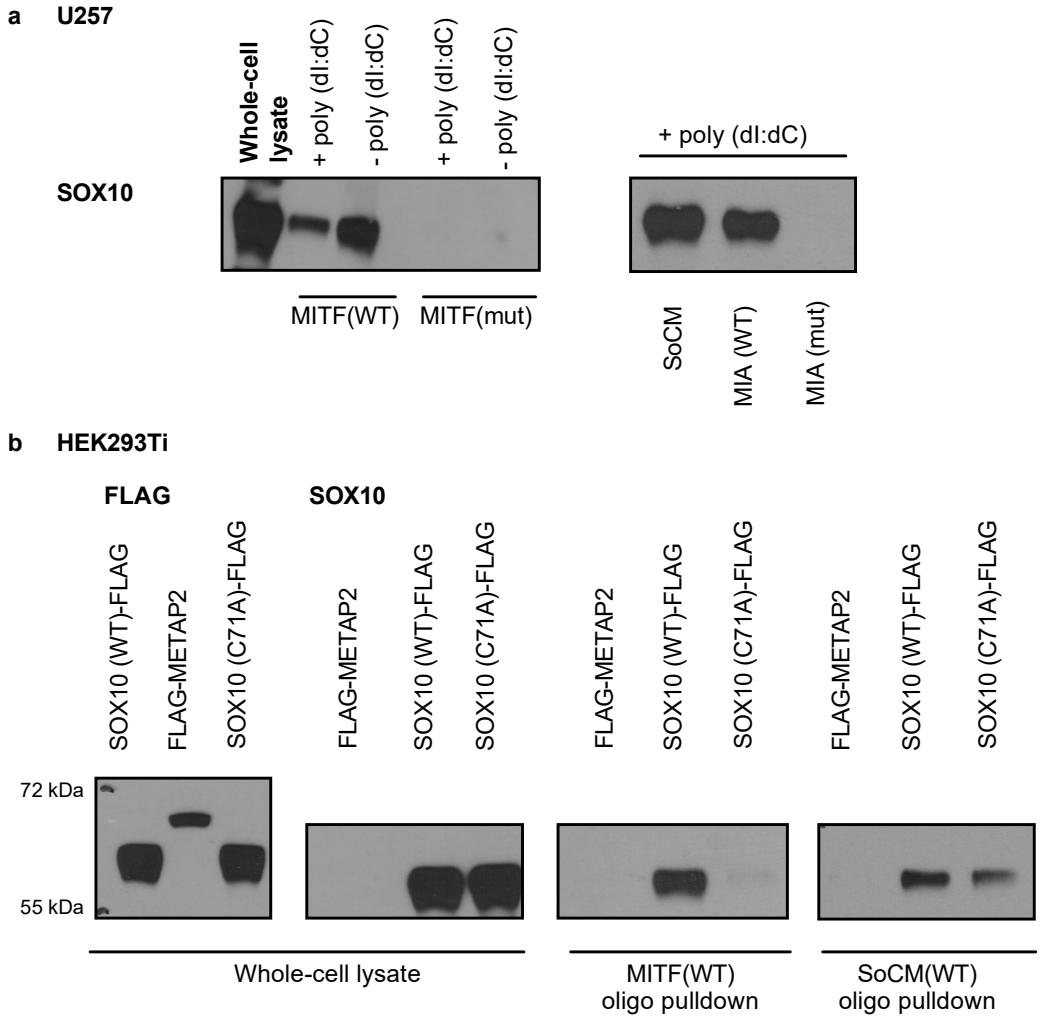

Figure 10: Oligonucleotide binding assays illustrate the disruption of SOX10 protein - target DNA binding following C71-mutation
a, Successful validation of oligonucleotides in U257. Endogenous SOX10 in U257 binds to MITF Wildtype (WT) promoter (40 bp sequence), SOX family consensus motif (SoCM) and MIA WT but does not bind to MITF-mutated (mut) promoter (40 bp) or MIA-mutated promotor. 400 µg of protein lysate was incubated with 30 µl of agarose beads that had been pre-incubated with 1 µg DNA. The western blot was stained with α-SOX10 (1:1000) from Cell Signaling Technology. Poly dI:dC is a synthetic, non-biotinylated competitor polymer used to capture non-specific DNA binding proteins. Adding poly dI:dC into the reaction decreased the SOX10 signal and was used in all succeeding oligonucleotide pulldown assays. **b,** l**eft** – FLAG: Confirming FLAG expression of transgene SOX10(WT)-FLAG, control FLAG-METAP2, and SOX10(C71A)-FLAG. The FLAG-tag consists of the amino acid sequence DYKDDDDK (1.012 kDa). Size of METAP: 67 kDa. **Right** - SOX10 expression in whole-cell lysate. Pulldown with MITF (WT) oligo shows that SOX10 (WT)-FLAG binds to MITF (WT), but SOX10 (C71A)-FLAG does not. After pulldown with SoCM, however, both WT and mut SOX10 show up. 4 µg plasmid / 10 cm dish was transfected. 400 µg protein and 30 µl oligo beads were used, α-FLAG, 1:1000, CST.

In summary, disturbed binding of SOX10 to mutated MITF validated the experimental setup and impaired binding of C71-mutated SOX10 to wildtype MITF, regulated by dimerized SOX10, suggested that their protein-DNA interaction depends on an intact C71. In contrast, mutating C71 did not show any effect on binding to the SOX10 consensus motif.

3.4 Cell proliferation experiments

Finally, cell proliferation experiments with the hit compound SH-0029 were performed to investigate its anticancer potential in several melanoma cell lines. By treating both SOX10-expressing and -dependent cell lines and those that neither express nor depend on SOX10 for their proliferation with SH-0029, the compound´s ability to act on-target was assessed. At 2.5 µM, cell proliferation was impaired in SOX10-positive more than in SOX10-negative melanoma cell lines **(Figure 11).**

To rule out general toxicity induced by the compound instead of cysteine-dependent degradation of SOX10 activity, ovarian cancer cell line (OVTOKO) was treated with the compound (40 / 20 / 10 / 5 / 2.5 µM) and showed no reduction in transcription activity (not shown). A luciferase reporter system based upon transcription factor PAX8 had been established.

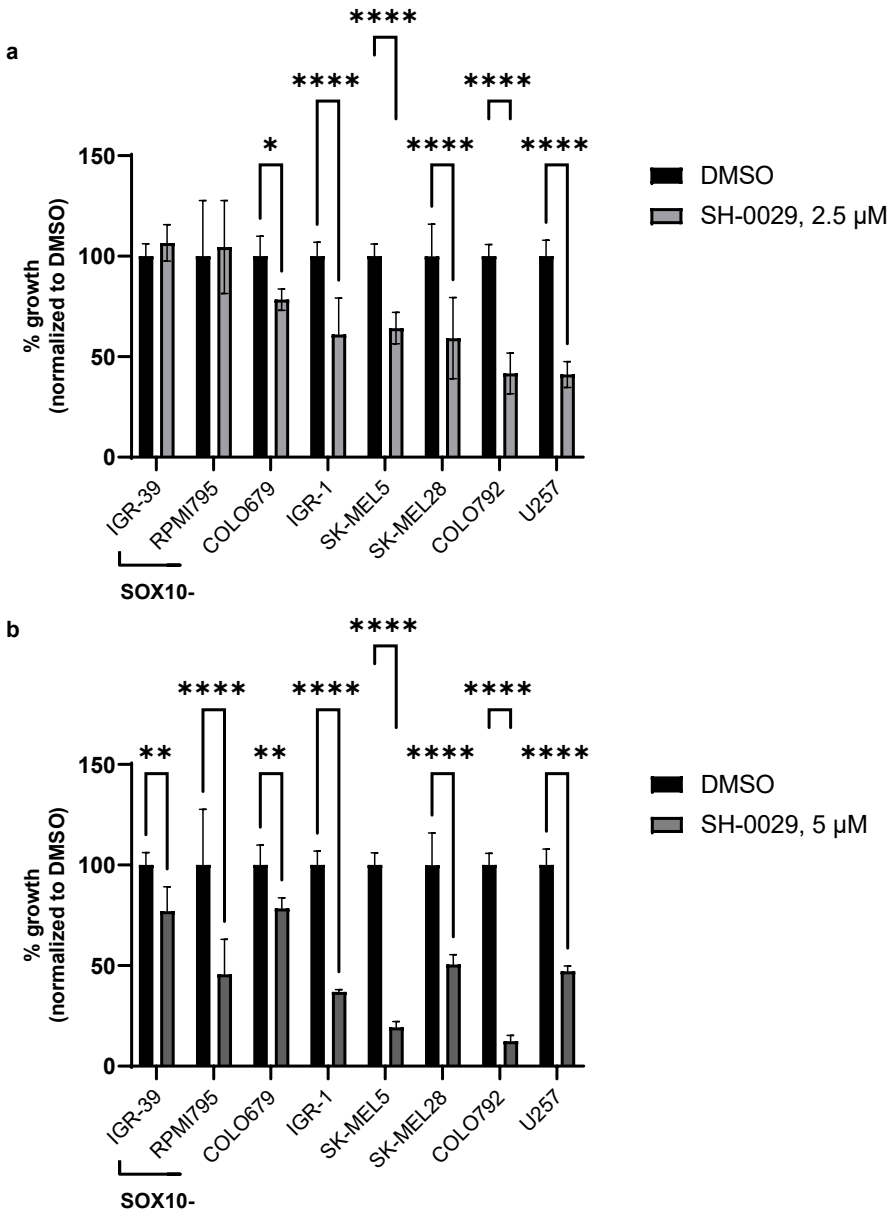

Figure 11: Cell proliferation experiments
a, At 2.5 µM, hit compound SH-0029 kills SOX10-dependent melanoma cells whereas SOX10-independent melanoma cells remain unaffected. **b,** At 5 µM, SH-0029 significantly decreases % growth in all cell lines, even the SOX10-negative cell lines IGR-39 and RPMI795.
Cells were plated in 96-well plates according to numbers plated in sgSOX10 experiments. Cells underwent a 3-day pretreatment, followed by a 6-day treatment, mimicking the schedule employed in growth assays. Cells were stained with 1 µg/ml Hoechst 33342 per each well. Results are displayed as means ± standard deviation, n = 10. Significance levels were determined using two-way ANOVA with Tukey´s post hoc test (*p<0.05, *p<0.01, ***p<0.001, ****p<0.0001.

4. Discussion

By knocking out SOX10 in several melanoma cell lines, its importance for cell proliferation was confirmed. A cysteine-reactive compound which decreased SOX10 transcriptional activity, and consequent expression of target genes, was identified. The hit compound´s mechanism of action was shown to be increased protein-protein interaction. In general, C71 proved crucial in protein-protein and protein-DNA interaction of the transcription factor.

4.1 SOX10´s role in proliferation of melanoma cells

SOX10-expressing melanoma cell lines showed significantly impaired proliferation when depleted of the transcription factor, demonstrating SOX10´s ability to sustain proliferative signaling. Cells that expressed SOX10 to a lower extent remained unaffected. SOX10 is a known dependency in melanoma cells and its essentiality was demonstrated by CRISPR and RNA interference (RNAi) data obtained by the Cancer Dependency Map at the Broad Institute (Broad Institute, 5/17/2024). Another study confirmed that silencing of SOX10 via small hairpin (sh) RNA repressed melanoma viability and clone formation in two cell lines (HT144 and A375) (Tang and Cao, 2021).

Herein, I implemented an sgRNA-guided knockout to study proliferation defects both qualitatively (microscopy) and quantitatively (growth assay). For the first time, 26 melanoma cell lines were profiled according to their dependency on SOX10 regarding their proliferation. In contrast to RNAi via shRNA, loss-of-function induced by CRISPR as used in this study is permanent.

4.2 SOX10 and MITF

An sgRNA-guided knockout of MITF caused significantly decreased cell viability in U257, whereas A375 continued to grow without visible changes. Previous studies have established that MITF is one of SOX10´s main target genes and high levels of MITF correlate with a proliferative, low levels with an invasive phenotype (Tudrej et al., 2017).

To study how SOX10 and MITF relate, I compared U257, a SOX10-high and MITF-high cell line, to A375, a SOX10-high but MITF-low cell line. It was shown that both cell lines depend on SOX10 regarding proliferation but loss of MITF did not bother A375. Taking together sgSOX10 and sgMITF-data, it follows that melanoma cell growth is primarily dependent on MITF in MITF-high cells, but in MITF-low cells SOX10 is required for growth.

4.3. Targeting SOX10, hit compound validation and its mechanism of action

By performing a large-scale screen of electrophilic compounds using MITF and TRPM promotor activity as a readout, two compounds were identified. It was shown that covalent adduction of the druggable cysteine in SOX10 resulted in functional impairment, i.e. disruption of protein-protein interaction, of the transcription factor.

In general, targeting transcription factors is challenging because protein-DNA and protein-protein interaction surfaces lack tractable active sites like the ones found in enzymes such as kinases. In transcription factors, DNA-protein interaction surfaces are usually convex and highly positively charged, protein-protein interaction sites are flat without any deep pockets (Bushweller, 2019). Whether a protein can be adducted by a ligand depends on the availability of a structural pocket for a small molecule to bind. In this study, a cysteine-reactive strategy was applied which allowed to specifically target cysteine residues by covalent, and therefore irreversible, binding.

There have been several efforts to inhibit SOX10 activity to date, mainly to analyze downstream effects. For example, knockdown of SOX10 revealed MIA downregulation and identified MIA as target gene of SOX10 (Graf et al., 2014). Another study employed an inhibitor to block lysine acetyltransferase (KAT) EP300, which is often co-amplified with SOX10 in melanoma. The inhibitor downregulated SOX10 protein levels, decreased proliferation and inhibited SOX10 signaling in SOX10-positive melanoma cells (Waddell et al., 2024). However, these genetic perturbations lack applicability, long-lasting effect and specificity to the transcription factor. Herein, a cysteine-reactive strategy was applied which allowed to specifically target the transcription factor and ensure irreversible binding between inhibiting compound and target region. Specificity of the inhibitor to SOX10 was

further confirmed by downregulation of SOX10 target genes, such as MITF and MIA, following compound treatment. Eight target genes were employed all of which were validated prior by siRNA-guided knockdown of SOX10.

It was then asked how the disturbance in transcriptional regulation was achieved by the compound. Herein, to study the specific interaction among SOX10 proteins, two types of SOX10 differing only by their amino acid tag (FLAG, HA) were expressed in a non-melanoma cell line. Co-immunoprecipitation allowed to pull down all FLAG-tagged SOX10 protein and show the protein fraction bound by it only. As expected, HA-tagged SOX10 was found to be specifically bound to FLAG-SOX10. Interestingly, hit compound treatment seemed to enforce protein-protein binding across different concentrations. It was therefore hypothesized that multimerization prevents active binding of the transcription factor to target DNA.

Succeeding experiments performed by Takahashi et al. (in the laboratory group of Liron Bar-Peled, PhD) later showed both in cells and in vitro that the protein-protein interaction induced by SH-0029 was dependent on an intact C71. Since SOX10 was initially picked up because of high cysteine-reactivity of C71 and the compound screen aimed at identifying an electrophilic molecule that covalently bound to that C71, it seems logical that without C71, hit compound treatment does not show the same effect. Additionally, it was hypothesized that in a C71A-mutant, SH-0029 should not be able to downregulate SOX10´s target genes and cellular proliferation. Further experiments by Takahashi et al. demonstrated that the proliferation block induced by SH-0029 could be rescued by expressing a C71A-mutant in U257 melanoma cells, compared to WT SOX10 (Takahashi et al., 2024).

4.4 SOX10´s mechanism of action

SOX10´s function was explored by analyzing oligonucleotide binding and protein-protein interaction. Comparison of compound-treated vs. DMSO-treated as well as C71A-mutated and -WT samples allowed to determine treatment- or mutation-related changes.

It is well known that SOXE family members including SOX8, SOX9 and SOX10 regulate gene expression mainly by dimerizing and that corresponding promotor regions to which these dimers bind encompass tandemly inverted consensus sequence (Peirano and Wegner, 2000). There a few studies dedicated to deciphering how the dimerization process works. Ramsook et al. hypothesized that the HMG domain itself might be involved in dimerization and were able to show interaction between a dimerization domain-like peptide and HMG-DNA. While they demonstrated that transcription factor SOX9 contains two amino acid residues essential to dimer formation, there has been no further analysis of SOX10´s dimerization domain (Ramsook et al., 2016). In addition, SOX10´s transcriptome and underlying gene regulatory network has been investigated thoroughly and allowed to cluster melanoma cell lines into melanocytic vs. mesenchymal subtypes (Wouters et al., 2020). Yet, differences in gene regulation by dimer or monomer formation of the transcription factor have not been fully understood.

In this study, it was found that a single mutation C71A disturbed binding of SOX10 to key target genes like MITF and MIA, both of which are known to be regulated by dimerized SOX10. Conversely, binding to a SOX10 monomer motif remained unchanged. It can therefore be hypothesized that C71 is crucial for dimerization-dependent gene regulation only.

Compound treatment decreased SOX10 transcriptional signaling as shown by qPCR experiments. It can therefore be hypothesized that disturbed SOX10 function, either by point mutation at C71 or increased multimerization of SOX10 induced by SH-0029, blocks downstream signaling and proliferation.

4.5 Future perspective / implications for further research

Future studies may explore in vivo applications of hit compounds. As this work is part of an ongoing project in the laboratory of Liron Bar-Peled, PhD, successful compounds are currently optimized, e.g., by altering and adjusting chemical moieties. As a result, similar treatment effects might be achieved at lower concentrations, thereby reducing cytotoxicity.

Data covering in vivo SOX10 inhibition is limited. There is a phenomenon that has occurred in prior in-vitro and in-vivo experiments after SOX10 inhibition called “phenotypic switching”. It is characterized by upregulation of SOX9 which leads to cellular transformation into a more invasive, mesenchymal state. In zebrafish, knockout of SOX10 reduced tumor incidence and SOX10 expression in those tumors that did develop but produced invasive melanomas which highly expressed SOX9 (Perlee et al., 2024). With the specificity of the cysteine-reactive inhibitors identified to SOX10, similar effects could be expected. Inhibition of SOX10 could potentially disrupt tumorigenesis of SOX10-expressing tumors but could still produce SOX9-expressing tumors with a rather different phenotype. Patient data obtained from The Cancer Genome Atlas (TCGA) linked high SOX9 expression to a significantly worse median survival rate of patients with metastatic melanoma (Cheng et al., 2015). In conclusion, undesirable effects of SOX10 depletion need to be explored thoroughly.

Apart from that, further mechanistic studies could be performed using an in-vitro binding assay. In-vitro binding, in contrast to the co-immunoprecipitation performed in cells, uses cell lysates which is why precise location and timing of SOX10 interaction would not have to be considered when treating with hit compounds. For example, in cells, SOX10 protein could have already formed a bond during / after translation off the ribosome in which case compound treatment would show no effect. In future experiments, hit compound treatment could be integrated into this assay.

Finally, while I focused on investigating SOX10 function on a molecular level, it would be interesting to further assess effects of the inhibitor. For example, SOX10 has been linked to melanoma invasion, mainly via genetic regulation of MIA (Graf et al., 2014). Activating

invasion and metastasis, like sustained proliferative signaling, belongs to the hallmarks of cancer (Hanahan, 2022) and melanoma states can be differentiated into proliferative or invasive. Studying how compound treatment affected cell migration in Matrigel or chick embryo invasion assays would allow for a broader understanding of SOX10´s role in melanoma.

4.6 Diagnostic opportunities

SOX10 is used as an immunohistochemical marker as it can detect metastatic melanoma in sentinel lymph nodes with high sensitivity. When compared to a panel of traditional immunohistochemical stains, e.g. S100, human melanoma black 45 (HMB-45) and Melan-A, SOX10 achieved statistically significant increases in both staining intensity and percentage of tumor cells stained (Willis et al., 2015). Evaluation of sentinel lymph node biopsy is considered the gold standard for the identification of early nodal metastasis in melanoma, determining a patient's prognosis and treatment (Faries et al., 2017). NCCN guidelines recommend SOX10 staining of sentinel lymph nodes (National Comprehensive Cancer Network, 2024).

Apart from that, an analysis of TCGA data correlated high SOX10 mRNA levels with poor prognosis (Tang and Cao, 2021). Potentially, SOX10 could be utilized as prognostic marker in the future.

4.7 Therapeutic considerations

Targeting SOX10 with a cysteine-reactive, electrophilic probe may ultimately result in the development of a clinically applicable drug. However, there are some findings that must be considered when implementing a SOX10-based therapy.

First, SOX10 plays an important role in the acquisition of stem cell features in melanoma cells by regulating CD-271, nestin and CD-133 expression. CD-271 influences self-renewal, chemo- and radiotherapy resistance. Nestin contributes to metastasis and CD-133

controls cell motility and invasion (Tudrej et al., 2017). When manipulating SOX10 function, stem-cell (-like) tumor cells will be targeted. Because tumor lesions consist of few cancer stem cells and mostly of non-stem cells, targeting SOX10 would have to be combined with a therapy for the bulk mass of non-stem cells, e.g. chemotherapy, immunotherapy, or radiotherapy.

Second, SOX10 loss promotes resistance against BRAF inhibitors. SOX10 depletion leads to an increase in TGFß signaling, which then raises EGFR and PDGFRß expression, which ultimately confers resistance to BRAF / MEK inhibitors (Han et al., 2018; Sun et al., 2014). This poses a challenge because patients with BRAF-mutated melanoma, which constitute roughly half of all melanoma patients, benefit from targeted therapy.

Third, resistance to BRAF / MEK inhibitors mediates resistance to immunotherapy. This might explain why in recent clinical trials administering targeted therapy before immunotherapy decreased efficacy of checkpoint inhibitors (e.g. DREAMSeq trial (Atkins et al., 2023)). It was shown that this cross-resistance is acquired throughout target therapy, arises from reactivated MAPK signaling and enables immune evasion through generating an immunosuppressive tumor microenvironment (Haas et al., 2021).

4.8 Targeting SOX10 in other tumor entities

The Cancer Dependency Map depicted SOX10 as gene of interest that is essential in cutaneous melanoma cell lines. Interestingly, similar essentiality was shown for SOX10 in several ocular melanoma cell lines, for example in OMM25, Chronos - 2.31, and one mucosal melanoma of the vagina / vulva cell line, (HMVII, Chronos - 2.2). Chronos scores measure the gene´s essentiality in a given cell line. More negative Chronos scores indicate a higher likelihood that the gene is essential, a Chronos score of zero would indicate that the gene is not essential. However, comparable Chronos scores were also calculated in tumor cell lines of the central nervous system, e.g., diffuse glioma cell lines LN229: - 3.11 and LN464: - 2.25) and breast cancer, not otherwise specified (NOS), e.g., COLO824 (- 2.54) (Broad Institute, 5/17/2024). This suggests that exploring SOX10 inhibition in cancers other than melanoma might be of interest.

SOX10 has been mentioned in other tumor entities already. For example, in triple-negative breast cancer, SOX10 has been reported as a reliable histopathological marker, adding to traditional breast cancer marker GATA-binding protein 3 (GATA3) (Jamidi et al., 2020). Another study compared expression profiles of triple-negative breast cancer tissue to adjacent healthy breast tissue. RNA-Sequencing showed that SOX10 expression was markedly elevated in the malignant tissue as well as MIA which was increased by 8.6-fold (Wu et al., 2021).

4.9 Limitations

There are two major limitations regarding the compound screen that could be addressed in future experimental setups.
First, apart from control cell lines OVTOKO, an ovarian cancer cell line, the entire screen was carried out in cell line U257. First, the cell line model in general is subject to limitations, for instance, it lacks microenvironment and additional cell types like fibroblasts, immune and endothelial cells. At least, among melanoma cell lines, U257 (= UACC257) was ranked amongst the top three cell lines that showed the highest transcriptional similarity when compared to their respective tumor counterparts (Vincent and Postovit, 2017). Second, the screen was carried out in a cell line that expresses comparably high levels of SOX10. U257 was selected for the screen because sgRNA-guided knockout was able to abolish SOX10 protein expression. However, by highly expressing SOX10 and MITF, U257 probably very sensitively identified hit compounds that decreased MITF promotor activity via inhibition of SOX10 transcriptional activity. Thereby, U257 represents MITF-high and therefore proliferative melanomas rather than invasive types. In future setups, adding melanoma cell lines of different subtypes will be critical.

Second, all results are based on a luciferase reporter that reads out SOX10 transcriptional activity via MITF promotor activity and MITF transcriptional activity via TRPM1 promotor activity, respectively. While MITF is the number one target gene and its interaction with SOX10 has been described extensively, using different target genes, like MIA, would be

interesting. This would allow to explore SOX10 signaling independent of MITF. In the future, implementation of ways to study transcription factor activity independent of the target gene should be helpful.

4.10 Conclusion

The role of SOX10 regarding melanoma initiation, proliferation and invasion had previously been reported. Yet, an in-depth understanding of how the transcription factor functions on a molecular level and strategies to disturb named mechanisms remained limited so far. This study now highlights SOX10´s role in melanoma proliferation leveraging CRISPR data and offers a novel strategy to identify and validate covalent inhibitors by integrating proteomic data with a high-throughput screen and functional assays. Covalent adduction of a druggable cysteine in SOX10 resulting in impaired signaling and melanoma cell proliferation prove the ligandability of SOX10 and establishes a model which might be translatable into tumor entities other than melanoma.

5. Summary

The project is based on cysteine druggability mapping data generated by Liron Bar-Peled, PhD, which unveiled a druggable cysteine in the dimerization domain of SOX10. This identified the transcriptional regulator as amenable to small-molecule covalent inactivation. The promising finding raised several questions concerning the role of SOX10 in melanoma cell lines, opportunities to identify electrophilic compounds targeting SOX10, and lastly, their underlying mechanism of action.

SOX10 depletion studies revealed an important role for the transcription factor in most melanoma cell lines: small-guide RNA (sgRNA) mediated knockout of SOX10 strongly attenuated the proliferation of SOX10 high expression cell lines, i.e., U257, but not of SOX10 low expression cells, i.e., RPMI795. Subsequently, a large-scale high-throughput screen was employed which yielded two promising hit compounds that mirrored the results of SOX10 depletion assays. Both were able to significantly decrease SOX10 transcriptional activity. When following up on these compounds, these results were reproducible in any SOX10-dependent melanoma cell line. qPCR analysis following compound treatment illustrated that hit compound treatment downregulated a majority of known SOX10 target genes, comparable to depleting the cell lines of SOX10.
C71 was confirmed as crucial for SOX10 function. When a point mutation (C71A) was introduced, protein-DNA binding was found to be compromised. Treatment with hit compound SH-0029, identified in the library screen, was shown to increase SOX10 multimerization and to downregulate target gene expression. This suggests that the compound specifically targets SOX10 and should lead to melanoma cell killing in SOX10-expressing cell lines. Cell proliferation assays confirmed compound-mediated cell killing in SOX10-dependent melanoma cell lines. These results indicate the potential to target SOX10, a transcription factor previously deemed as intractable, thereby giving way to novel treatment approaches.

6. List of figures

7. List of tables

8. References

Ascierto PA, McArthur GA, Dréno B, Atkinson V, Liszkay G, Di Giacomo AM, Mandalà M, Demidov L, Stroyakovskiy D, Thomas L, La Cruz-Merino L de, Dutriaux C, Garbe C, Yan Y, Wongchenko M, Chang I, Hsu JJ, Koralek DO, Rooney I, Ribas A, Larkin J. Cobimetinib combined with vemurafenib in advanced BRAFV600-mutant melanoma (coBRIM): updated efficacy results from a randomised, double-blind, phase 3 trial. Lancet Oncol 2016; 17: 1248–1260

Atkins MB, Lee SJ, Chmielowski B, Tarhini AA, Cohen GI, Truong T-G, Moon HH, Davar D, O'Rourke M, Stephenson JJ, Curti BD, Urba WJ, Brell JM, Funchain P, Kendra KL, Ikeguchi AP, Jaslowski A, Bane CL, Taylor MA, Bajaj M, Conry RM, Ellis RJ, Logan TF, Laudi N, Sosman JA, Crockett DG, Pecora AL, Okazaki IJ, Reganti S, Chandra S, Guild S, Chen HX, Streicher HZ, Wolchok JD, Ribas A, Kirkwood JM. Combination Dabrafenib and Trametinib Versus Combination Nivolumab and Ipilimumab for Patients With Advanced BRAF -Mutant Melanoma: The DREAMseq Trial—ECOG-ACRIN EA6134. J Clin Oncol 2023; 41: 186–197

Bar-Peled L, Kemper EK, Suciu RM, Vinogradova EV, Backus KM, Horning BD, Paul TA, Ichu T-A, Svensson RU, Olucha J, Chang MW, Kok BP, Zhu Z, Ihle NT, Dix MM, Jiang P, Hayward MM, Saez E, Shaw RJ, Cravatt BF. Chemical Proteomics Identifies Druggable Vulnerabilities in a Genetically Defined Cancer. Cell 2017; 171: 696-709.e23

Boike L, Henning NJ, Nomura DK. Advances in covalent drug discovery. Nat Rev Drug Discov 2022; 21: 881–898

Bowles J, Schepers G, Koopman P. Phylogeny of the SOX family of developmental transcription factors based on sequence and structural indicators. Dev Biol 2000; 227: 239–255

Broad Institute, 2024: SOX10 DepMap Gene Summary. available online https://depmap.org/portal/gene/SOX10?tab=dependency (date of access 5 /17/2024)

Bushweller JH. Targeting transcription factors in cancer - from undruggable to reality. Nat Rev Cancer 2019; 19: 611–624

Cheng L, Lopez-Beltran A, Massari F, MacLennan GT, Montironi R. Molecular testing for BRAF mutations to inform melanoma treatment decisions: a move toward precision medicine. Mod Pathol 2018; 31: 24–38

Cheng PF, Shakhova O, Widmer DS, Eichhoff OM, Zingg D, Frommel SC, Belloni B, Raaijmakers MI, Goldinger SM, Santoro R, Hemmi S, Sommer L, Dummer R, Levesque MP. Methylation-dependent SOX9 expression mediates invasion in human melanoma cells and is a negative prognostic factor in advanced melanoma. Genome Biol 2015; 16: 42

Copeland RA. The drug-target residence time model: a 10-year retrospective. Nat Rev Drug Discov 2016; 15: 87–95

Dummer R, Ascierto PA, Gogas HJ, Arance A, Mandala M, Liszkay G, Garbe C, Schadendorf D, Krajsova I, Gutzmer R, Chiarion Sileni V, Dutriaux C, Groot JWB de, Yamazaki N, Loquai C, Moutouh-de Parseval LA, Pickard MD, Sandor V, Robert C, Flaherty KT. Overall

survival in patients with BRAF-mutant melanoma receiving encorafenib plus binimetinib versus vemurafenib or encorafenib (COLUMBUS): a multicentre, open-label, randomised, phase 3 trial. Lancet Oncol 2018; 19: 1315–1327

Faries MB, Thompson JF, Cochran AJ, Andtbacka RH, Mozzillo N, Zager JS, Jahkola T, Bowles TL, Testori A, Beitsch PD, Hoekstra HJ, Moncrieff M, Ingvar C, Wouters MWJM, Sabel MS, Levine EA, Agnese D, Henderson M, Dummer R, Rossi CR, Neves RI, Trocha SD, Wright F, Byrd DR, Matter M, Hsueh E, MacKenzie-Ross A, Johnson DB, Terheyden P, Berger AC, Huston TL, Wayne JD, Smithers BM, Neuman HB, Schneebaum S, Gershenwald JE, Ariyan CE, Desai DC, Jacobs L, McMasters KM, Gesierich A, Hersey P, Bines SD, Kane JM, Barth RJ, McKinnon G, Farma JM, Schultz E, Vidal-Sicart S, Hoefer RA, Lewis JM, Scheri R, Kelley MC, Nieweg OE, Noyes RD, Hoon DSB, Wang H-J, Elashoff DA, Elashoff RM. Completion Dissection or Observation for Sentinel-Node Metastasis in Melanoma. N Engl J Med 2017; 376: 2211–2222

Ferrucci PF, Di Giacomo AM, Del Vecchio M, Atkinson V, Schmidt H, Schachter J, Queirolo P, Long GV, Stephens R, Svane IM, Lotem M, Abu-Amna M, Gasal E, Ghori R, Diede SJ, Croydon ES, Ribas A, Ascierto PA. KEYNOTE-022 part 3: a randomized, double-blind, phase 2 study of pembrolizumab, dabrafenib, and trametinib in BRAF-mutant melanoma. J Immunother Cancer 2020; 8: e001806

Flammiger A, Besch R, Cook AL, Maier T, Sturm RA, Berking C. SOX9 and SOX10 but not BRN2 are required for nestin expression in human melanoma cells. J Invest Dermatol 2009; 129: 945–953

Fufa TD, Harris ML, Watkins-Chow DE, Levy D, Gorkin DU, Gildea DE, Song L, Safi A, Crawford GE, Sviderskaya EV, Bennett DC, Mccallion AS, Loftus SK, Pavan WJ. Genomic analysis reveals distinct mechanisms and functional classes of SOX10-regulated genes in melanocytes. Hum Mol Genet 2015; 24: 5433–5450

Göhl J, Hohenberger W, Merkel S. Malignes Melanom. Chirurg 2009; 80: 559–567

Graf SA, Busch C, Bosserhoff A-K, Besch R, Berking C. SOX10 promotes melanoma cell invasion by regulating melanoma inhibitory activity. J Invest Dermatol 2014; 134: 2212–2220

Gutzmer R, Stroyakovskiy D, Gogas H, Robert C, Lewis K, Protsenko S, Pereira RP, Eigentler T, Rutkowski P, Demidov L, Manikhas GM, Yan Y, Huang K-C, Uyei A, McNally V, McArthur GA, Ascierto PA. Atezolizumab, vemurafenib, and cobimetinib as first-line treatment for unresectable advanced BRAFV600 mutation-positive melanoma (IMspire150): primary analysis of the randomised, double-blind, placebo-controlled, phase 3 trial. Lancet Oncol 2020; 395: 1835–1844

Haas L, Elewaut A, Gerard CL, Umkehrer C, Leiendecker L, Pedersen M, Krecioch I, Hoffmann D, Novatchkova M, Kuttke M, Neumann T, Da Silva IP, Witthock H, Cuendet MA, Carotta S, Harrington KJ, Zuber J, Scolyer RA, Long GV, Wilmott JS, Michielin O, Vanharanta S, Wiesner T, Obenauf AC. Acquired resistance to anti-MAPK targeted therapy confers an immune-evasive tumor microenvironment and cross-resistance to immunotherapy in melanoma. Nat Cancer 2021; 2: 693–708

Han S, Ren Y, He W, Liu H, Zhi Z, Zhu X, Yang T, Rong Y, Ma B, Purwin TJ, Ouyang Z, Li C, Wang X, Wang X, Yang H, Zheng Y, Aplin AE, Liu J, Shao Y. ERK-mediated phosphorylation regulates SOX10 sumoylation and targets expression in mutant BRAF melanoma. Nat Commun 2018; 9: 28

Hanahan D. Hallmarks of Cancer: New Dimensions. Cancer Discov 2022; 12: 31–46

Jamidi SK, Hu J, Aphivatanasiri C, Tsang JY, Poon IK, Li JJ, Chan S-K, Cheung S-Y, Tse GM. Sry-related high-mobility-group/HMG box 10 (SOX10) as a sensitive marker for triple-negative breast cancer. Histopathology 2020; 77: 936–948

Jessurun CAC, Vos JAM, Limpens J, Luiten RM. Biomarkers for Response of Melanoma Patients to Immune Checkpoint Inhibitors: A Systematic Review. Front Oncol 2017; 7: 233

Larkin J, Chiarion-Sileni V, Gonzalez R, Grob J-J, Rutkowski P, Lao CD, Cowey CL, Schadendorf D, Wagstaff J, Dummer R, Ferrucci PF, Smylie M, Hogg D, Hill A, Márquez-Rodas I, Haanen J, Guidoboni M, Maio M, Schöffski P, Carlino MS, Lebbé C, McArthur G, Ascierto PA, Daniels GA, Long GV, Bastholt L, Rizzo JI, Balogh A, Moshyk A, Hodi FS, Wolchok JD. Five-Year Survival with Combined Nivolumab and Ipilimumab in Advanced Melanoma. N Engl J Med 2019; 381: 1535–1546

Larouche K, Bergeron MJ, Leclerc S, Guérin SL. Optimization of competitor poly(dI-dC).poly(dI-dC) levels is advised in DNA-protein interaction studies involving enriched nuclear proteins. Biotechniques 1996; 20: 439–444

Matthews NH, Li W-Q, Qureshi AA, Weinstock MA, Cho E: Epidemiology of Melanoma. in: Ward WH, Farma JM (eds): Cutaneous Melanoma: Etiology and Therapy Brisbane (AU): Codon Publications, 2017: 3-22

Maurais AJ, Weerapana E. Reactive-cysteine profiling for drug discovery. Curr Opin Chem Biol 2019; 50: 29–36

Michielin O, van Akkooi ACJ, Ascierto PA, Dummer R, Keilholz U. Cutaneous melanoma: ESMO Clinical Practice Guidelines for diagnosis, treatment and follow-up†. Ann Oncol 2019; 30: 1884–1901

Miller AJ, Du J, Rowan S, Hershey CL, Widlund HR, Fisher DE. Transcriptional regulation of the melanoma prognostic marker melastatin (TRPM1) by MITF in melanocytes and melanoma. Cancer Res 2004; 64: 509–516

Nathan P, Dummer R, Long GV, Ascierto PA, Tawbi HA, Robert C, Rutkowski P, Leonov O, Dutriaux C, Mandala' M, Lorigan P, Ferrucci PF, Flaherty KT, Brase JC, Green S, Haas T, Masood A, Gasal E, Ribas A, Schadendorf D. LBA43 Spartalizumab plus dabrafenib and trametinib (Sparta-DabTram) in patients (pts) with previously untreated BRAF V600–mutant unresectable or metastatic melanoma: Results from the randomized part 3 of the phase III COMBI-i trial. Ann Oncol 2020; 31: S1172

National Comprehensive Cancer Network, 2024: NCCN Clinical Practical Guidelines in Oncology (NCCN Guidelines®) Melanoma: Cutaneous 2024. available online https://www.nccn.org/guidelines/guidelines-detail?category=1&id=1492 (date of access: 5/5/2024)

Leitlinienprogramm Onkologie (Deutsche Krebsgesellschaft, Deutsche Krebshilfe, AWMF): Diagnostik, Therapie und Nachsorge des Melanoms, Langversion 3.3, 2020,

AWMF Registernummer: 032/024OL, available online http://www.leitlinienprogrammonkologie.de/leitlinien/melanom/ (date of access: 5/10/2024)

Peirano RI, Wegner M. The glial transcription factor Sox10 binds to DNA both as monomer and dimer with different functional consequences. Nucleic Acids Res 2000; 28: 3047–3055

Perlee S, Ma Y, Hunter MV, Swanson JB, Ming Z, Xia J, Lionnet T, McGrail M, White R. A zebrafish system for identifying genetic dependencies in melanocytes and melanoma. bioRxiv 2024 [Preprint]

Pingault V, Zerad L, Bertani-Torres W, Bondurand N. SOX10: 20 years of phenotypic plurality and current understanding of its developmental function. J Med Genet 2022; 59: 105–114

Ramsook SN, Ni J, Shahangian S, Vakiloroayaei A, Khan N, Kwan JJ, Donaldson LW. A Model for Dimerization of the SOX Group E Transcription Factor Family. PLoS One 2016; 11: e0161432

Robert Koch-Institut, Gesellschaft der epidemiologischen Krebsregister in Deutschland e.V., 2023: Krebs in Deutschland für 2019/2020. 14th edition. available online https://www.krebsdaten.de/Krebs/DE/Content/Publikationen/Krebs_in_Deutschland/krebs_in_deutschland_2023.pdf?__blob=publicationFile (date of access: 5/5/2024)

Robert C, Grob JJ, Stroyakovskiy D, Karaszewska B, Hauschild A, Levchenko E, Chiarion Sileni V, Schachter J, Garbe C, Bondarenko I, Gogas H, Mandalá M, Haanen JBAG, Lebbé C, Mackiewicz A, Rutkowski P, Nathan PD, Ribas A, Davies MA, Flaherty KT, Burgess P, Tan M, Gasal E, Voi M, Schadendorf D, Long GV. Five-Year Outcomes with Dabrafenib plus Trametinib in Metastatic Melanoma. N Engl J Med 2019a; 381: 626–636

Robert C, Ribas A, Schachter J, Arance A, Grob J-J, Mortier L, Daud A, Carlino MS, McNeil CM, Lotem M, Larkin JMG, Lorigan P, Neyns B, Blank CU, Petrella TM, Hamid O, Su S-C, Krepler C, Ibrahim N, Long GV. Pembrolizumab versus ipilimumab in advanced melanoma (KEYNOTE-006): post-hoc 5-year results from an open-label, multicentre, randomised, controlled, phase 3 study. Lancet Oncol 2019b; 20: 1239–1251

Rodríguez-Cerdeira C, Carnero Gregorio M, López-Barcenas A, Sánchez-Blanco E, Sánchez-Blanco B, Fabbrocini G, Bardhi B, Sinani A, Guzman RA. Advances in Immunotherapy for Melanoma: A Comprehensive Review. Mediators Inflamm 2017; 2017: 3264217

Subbiah V, Baik C, Kirkwood JM. Clinical Development of BRAF plus MEK Inhibitor Combinations. Trends Cancer 2020; 6: 797–810

Sun C, Wang L, Huang S, Heynen GJJE, Prahallad A, Robert C, Haanen J, Blank C, Wesseling J, Willems SM, Zecchin D, Hobor S, Bajpe PK, Lieftink C, Mateus C, Vagner S, Grernrum W, Hofland I, Schlicker A, Wessels LFA, Beijersbergen RL, Bardelli A, Di Nicolantonio F, Eggermont AMM, Bernards R. Reversible and adaptive resistance to BRAF(V600E) inhibition in melanoma. Nature 2014; 508: 118–122

Sutanto F, Konstantinidou M, Dömling A. Covalent inhibitors: a rational approach to drug discovery. RSC Med Chem 2020; 11: 876–884

Takahashi M, Chong HB, Zhang S, Yang T-Y, Lazarov MJ, Harry S, Maynard M, Hilbert B, White RD, Murrey HE, Tsou C-C, Vordermark K, Assaad J, Gohar M, Dürr BR, Richter

M, Patel H, Kryukov G, Brooijmans N, Alghali ASO, Rubio K, Villanueva A, Zhang J, Ge M, Makram F, Griesshaber H, Harrison D, Koglin A-S, Ojeda S, Karakyriakou B, Healy A, Popoola G, Rachmin I, Khandelwal N, Neil JR, Tien P-C, Chen N, Hosp T, van den Ouweland S, Hara T, Bussema L, Dong R, Shi L, Rasmussen MQ, Domingues AC, Lawless A, Fang J, Yoda S, Nguyen LP, Reeves SM, Wakefield FN, Acker A, Clark SE, Dubash T, Kastanos J, Oh E, Fisher DE, Maheswaran S, Haber DA, Boland GM, Sade-Feldman M, Jenkins RW, Hata AN, Bardeesy NM, Suvà ML, Martin BR, Liau BB, Ott CJ, Rivera MN, Lawrence MS, Bar-Peled L. DrugMap: A quantitative pan-cancer analysis of cysteine ligandability. Cell 2024; 187: 2536-2556.e30

Tang Y, Cao Y. SOX10 Knockdown Inhibits Melanoma Cell Proliferation via Notch Signaling Pathway. Cancer Manag Res 2021; 13: 7225–7234

Trojaniello C, Sparano F, Cioli E, Ascierto PA. Sequencing Targeted and Immune Therapy in BRAF-Mutant Melanoma: Lessons Learned. Curr Oncol Rep 2023; 25: 623–634

Tudrej KB, Czepielewska E, Kozłowska-Wojciechowska M. SOX10-MITF pathway activity in melanoma cells. Arch Med Sci 2017; 13: 1493–1503

Vincent KM, Postovit L-M. Investigating the utility of human melanoma cell lines as tumour models. Oncotarget 2017; 8: 10498–10509

Vinogradova EV, Cravatt BF. Multiplexed proteomic profiling of cysteine reactivity and ligandability in human T cells. STAR Protoc 2021; 2: 100458

Waddell A, Grbic N, Leibowitz K, Wyant WA, Choudhury S, Park K, Collard M, Cole PA, Alani RM. p300 KAT regulates SOX10 stability and function in human melanoma. Cancer Res Commun. 2024;4(8):1894-1907.

Wahlbuhl M, Reiprich S, Vogl MR, Bösl MR, Wegner M. Transcription factor Sox10 orchestrates activity of a neural crest-specific enhancer in the vicinity of its gene. Nucleic Acids Res 2012; 40: 88–101

Willis BC, Johnson G, Wang J, Cohen C. SOX10: a useful marker for identifying metastatic melanoma in sentinel lymph nodes. Appl Immunohistochem Mol Morphol 2015; 23: 109–112

Wouters J, Kalender-Atak Z, Minnoye L, Spanier KI, Waegeneer M de, Bravo González-Blas C, Mauduit D, Davie K, Hulselmans G, Najem A, Dewaele M, Pedri D, Rambow F, Makhzami S, Christiaens V, Ceyssens F, Ghanem G, Marine J-C, Poovathingal S, Aerts S. Robust gene expression programs underlie recurrent cell states and phenotype switching in melanoma. Nat Cell Biol 2020; 22: 986–998

Wu W, Warner M, Wang L, He W-W, Zhao R, Guan X, Botero C, Huang B, Ion C, Coombes C, Gustafsson J-A. Drivers and suppressors of triple-negative breast cancer. Proc Natl Acad Sci U S A 2021; 118

Zhang H. Osimertinib making a breakthrough in lung cancer targeted therapy. Onco Targets Ther 2016; 9: 5489–5493

9. Acknowledgements

I would like to express my sincere gratitude to Prof. Schmidt-Wolf, University of Bonn, Germany and Liron-Bar-Peled, PhD, Assistant Professor, Harvard Medical School, Boston, USA, for their support at every stage of the research project.